The Dissertation Committee for Alexander Edward Primus certifies that this is the approved version of the following dissertation:

Regional specification in the early embryo of the

brittle star *Ophiopholis aculeata*

Committee:

_____

Gary Freeman, Supervisor

_____

David Parichy

_____

Marty Shankland

_____

James Sprinkle

_____

David Stein

Regional specification in the early embryo of the

brittle star *Ophiopholis aculeata*

by

Alexander Edward Primus, B.A.

Dissertation

Presented to the Faculty of the Graduate School of

The University of Texas at Austin

in Partial Fulfillment

of the Requirements

for the Degree of

Doctor of Philosophy

The University of Texas at Austin

May 2005

Acknowledgments

Many people have helped my complete this project. First and foremost I would like to thank my advisor Gary Freeman. Gary has trained me think as an experimental embryologist, taught me techniques used to manipulate and rear marine invertebrate embryos, advised me on how to present my work, and supported me intellectually and financially throughout my graduate career. I thank the NSF for their financial support (grant IBN 9982024 to Gary Freeman). I would like to thank my committee members for their thoughtful insight. My committee was composed of Dr. David Parichy, Dr. Marty Shankland, Dr. David Stein, Dr. James Sprinkle, and my advisor Dr. Gary Freeman.

I also thank many members of the Friday Harbor Labs (FHL) community who have helped me by providing technical assistance, engaging in thoughtful discussion, contributing reagents, assisting in animal collection, caring for animals, and/or being good company. These people include George von Dassow, Richard Strathmann, Kirk Zigler, Eric Edsinger-Gonzales, Sean Cain, Bruno Pernet, Mike Baltzley, Jon Allen, Paul Bordeaux, Kimberly Porter, Federico Brown, Mickey von Dassow, Russell Wyeth, Alison Sweeny, Molly Jacobs, Tammy McGovern, Steph Porter, Fernanda Oyarzun, Roddy Foley, Kevin Britten-Simmons, Ryan Gile, Svetlana Maslakova, Mark Q. Martindale, Russel Zimmer, Steve Stricker, Charlie Lambert, and Billie Swalla. I thank the director of the Friday Harbor Laboratories Dennis Willows for allowing me to conduct my research at FHL, Blanche Bybee, Amiee Urata, Craig Staude and the

remainder of the FHL support staff, and the Center for Cell Dynamics at the FHL for the very generous use of their confocal and fluorescence dissection microscopes.

Finally, I would like to thank my parents who have been very supportive of me and my pursuits throughout my life.

Regional specification in the early embryo of the

brittle star *Ophiopholis aculeata*

Publication No. _____

Alexander Edward Primus, Ph.D.
University of Texas at Austin, 2005

Supervisor: Gary Freeman

Early embryogenesis has been examined experimentally in four of the seven echinoderm and hemichordate classes. Although these studies suggest that the mechanisms which underlie regional specification have been highly conserved within the echinoderm + hemichordate clade, nothing is known about these mechanisms within the other echinoderm classes, including the Ophiuroidea. In this study, early embryogenesis was examined in the ophiuroid *Ophiopholis aculeata*. Several aspects of early development in this ophiuroid differ from those of other echinoderms and hemichordates. In *O. aculeata*, the first two cleavage planes do not coincide with the animal-vegetal axis but rather form approximately 45 degrees off this axis. Fate maps of 2-, 4- and 8-cell embryos were constructed using microinjected lineage tracers and indicate that ectoderm, endoderm, and mesoderm segregate unequally at first cleavage. The distribution of

developmental potential in the embryo was examined by isolating different regions of the early embryo and indicate that endomesodermal developmental potential segregates unequally at first, second, and third cleavage. In other echinoderm and hemichordate embryos, similar unequal segregations of larval fates and developmental potential typically do not occur until third cleavage. These results indicate that there has been an evolutionary shift in the orientation of the early cleavage program in *O. aculeata* with respect to the distribution of larval fates and developmental potential.

Experiments were also performed to gain insight into the molecular mechanisms which underlie axial specification in *O. aculeata*. Evidence for a role of nuclear β-catenin was assessed by examining its localization and by perturbing its activity. β-catenin localization was observed during gastrula-stages when it was seen in adherens junctions of epithelial cells; there was no indication of any nuclear localization of β-catenin throughout embryogenesis. Treatment of embryos with LiCl (an inhibitor of β-catenin degradation) produced results largely inconsistent with its role in endomesodermal specification. Dorsal-ventral patterning mechanisms were investigated by treating embryos with $NiCl_2$ (which radialize echinoid embryos, potentially by disrupting TGFβ signaling). Nickel-treatment disrupted ectodermal development but never radialized embryos completely. These results suggest that the molecular mechanisms of axial specification in *O. aculeata* may differ from those of echinoid embryos.

Table of Contents

Chapter 1: General Introduction

Regional and cell-fate specification, the processes by which different cells or regions of a developing embryo acquire their developmental fates, have been subjects of biological research since the late 19th century. Investigations in embryological and developmental genetic model systems have taught us a great deal about the cellular, molecular, and genetic basis for these processes. Comparisons between these systems have uncovered several themes regarding the evolution of developmental mechanisms (Gerhart and Kirschner, 1997; Raff, 1996). One major finding of these comparisons is that a hypothetical 'developmental toolbox' appears to exist in which numerous developmental tools reside. Many of these tools, which include various diffusible signaling molecules, intracellular signaling pathways and transcriptional regulators, have clearly been used multiple times during the course of metazoan evolution to mediate a plethora of developmental functions within and between animal taxa.

The use of non-model systems has also contributed to our understanding of the interface between development and evolution. A great deal of work has focused on comparisons made between closely related groups (i.e. at the level of genus or species). These studies have taught us a great deal about developmental changes that occur at the micro-evolutionary scale. Despite this, very little is known about how specification mechanisms associated with early embryogenesis evolve at the level of class and phylum. To gain insight into the evolution of developmental mechanisms at the class level, I have

examined embryogenesis in one class of echinoderms and compared that to embryogenesis in other closely related classes. Echinoderms represent an ideal system with which to examine the evolution of regional specification between classes for a number of reasons: 1) Because echinoid embryos have been a model system for developmental studies, a great deal is already known about the mechanisms that underlie early development and regional specification in this group (Angerer and Angerer, 2003; Davidson *et al.*, 2002; Ettensohn and Sweet, 2000). 2) Paleontological and molecular phylogenetic data have revealed a great deal regarding the phylogenetic affinities of this group. 3) Members of each extant echinoderm classes develop indirectly via free-swimming planktonic larvae. 4) Echinoderm embryos from all five extant classes are easy to obtain and most are amenable to experimental manipulation. 5) Because all five extant echinoderm classes were present by the Ordovician (Smith, 1988), these groups are potentially quite divergent.

Phylogenetic affinities of echinoderm classes

The phylum Echinodermata is composed of five extant classes: Echinoidea, Holothuroidea, Asteroidea, Ophiuroidea, and Crinoidea (Hyman, 1955). Current molecular phylogenies indicate that the Echinodermata form a monophyletic clade with the Hemichordata; together, these two phyla contain all non-chordate deuterostomes (Cameron *et al.*, 2000; Winchell *et al.*, 2002). Several class-level phylogenies of extant echinoderms have been constructed in the past 25 years. The most recent and comprehensive of these analyses (which are based on morphological data, molecular

2

data, or a combination of both) strongly support a scenario in which the crinoids are the most basal members of the group (Fig. 1.1A) (Littlewood *et al.*, 1997; Smith, 1997; Sumrall and Sprinkle, 1998). Most analyses also suggest that the echinoids and holothuroids are sister taxa. The placement of the asteroids and ophiuroids, based on these analyses, is less certain. The following three hypotheses are all well supported: 1) the ophiuroids and asteroids form a clade which is a sister-group to the echinoid + holothuroid clade (Fig. 1.1B), 2) the ophiuroids are a sister-group to the echinoid + holothuroid clade (Fig. 1.1C), or 3) the asteroids are a sister-group to the echinoid + holothuroid clade (Fig. 1.1D). Analyses using mitochondrial gene order have been unable to resolve this issue (Scouras and Smith, 2001; Scouras *et al.*, 2004; Smith *et al.*, 1993).

Echinoid embryogenesis and larval development

Because much of what is known about the development of echinoderms is based on studies of echinoids, the development of a typical sea urchin echinopluteus larva will be briefly described. In the sea urchin, fertilization is followed by an early period of cell divisions. Early cell divisions are typically equal (Fig. 1.2A), but during the fourth round of cytokinesis, cells in the vegetal half of the embryo cleave unequally and produce 4 small micromeres and 4 large macromeres (Fig. 1.2B); this is generally thought to be a derived feature since the 4th cleavage is equal in the all other extant echinoderm classes. Basal extant echinods such as *Eucidaris* may represent a transitional phase in the move from equal to unequal 4th cleavage since they typically only form 2-3 micromeres at 4th
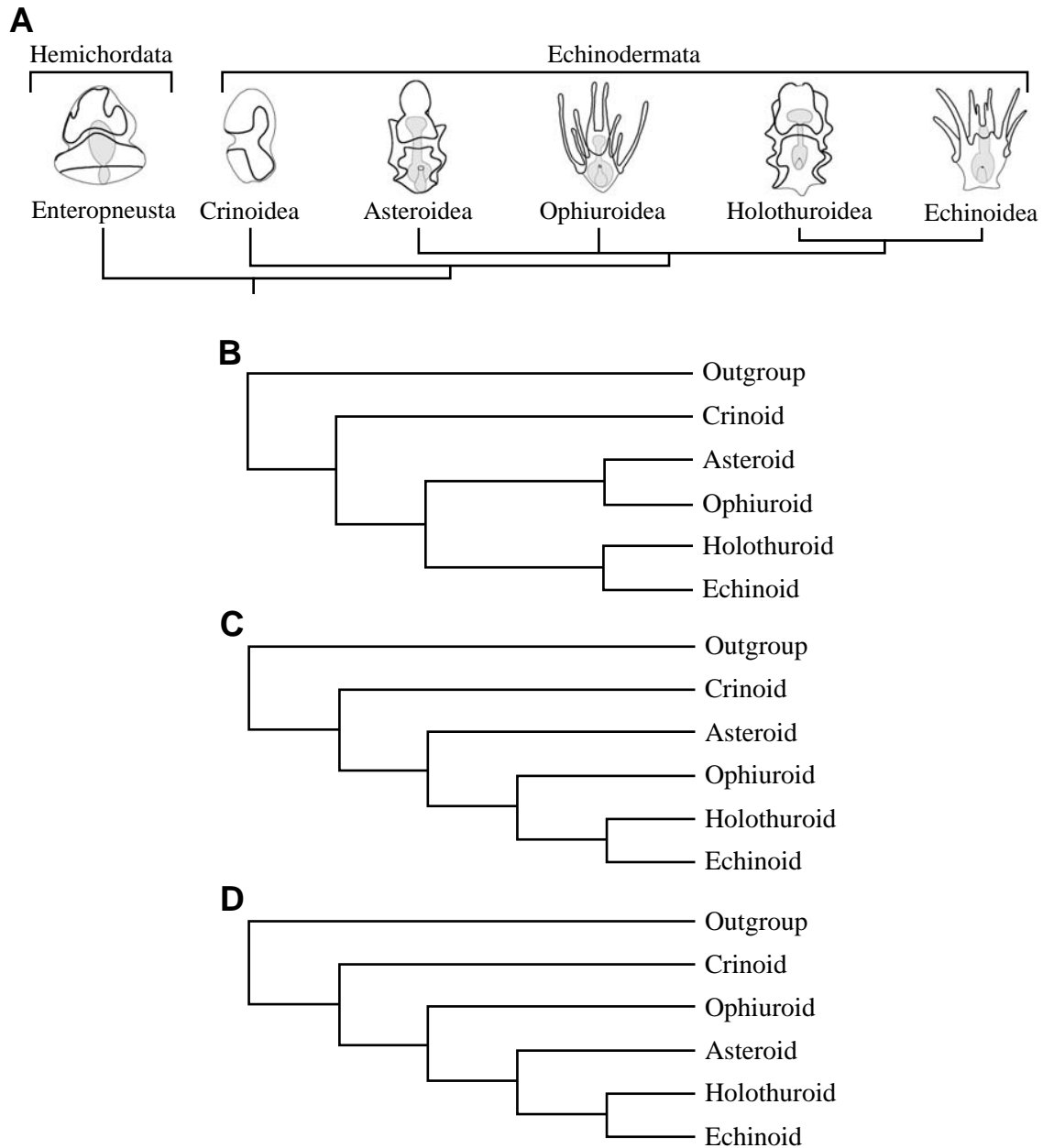
3

Fig. 1.1. Phylogenies of extant echinoderm classes. (A) Larval forms of extant echinoderm classes with an enteropneust hemichordate out-group. Echinoids and ophiuroids are the only groups which develop via the production of a pluteus larva (which bear long ciliated arms supported by a larval skeleton). (B-D) Three best-supported, fully-resolved phylogenies of extant echinoderm classes. Based on Littlewood *et al*., (1997) and Cameron *et al*., (2000).

cleavage and these cells are proportionately larger than normal micromeres (Schroeder, 1981). The initial period of cell divisions ultimately ends in the formation of a hollow blastula (Fig. 1.2C). Next, the vegetal-most cells of the blastula elongate apico-basally to produce a thickened vegetal plate, from which several cells ingress into the blastocoel (Fig. 1.2D). These ingressing cells, called primary mesenchyme cells (PMCs), are derived from the 4 micromeres produced at the 16-cell stage and will ultimately produce a larval skeleton. Following PMC ingression, gastrulation commences as the cells of the floorplate invaginate to produce an archenteron (Fig. 1.2E-G). The archenteron subsequently elongates and fuses with ectodermal cells, thereby forming a tri-partite larval through gut (Fig. 1.2H). Simultaneous with archenteron elongation, several cells of the archenteron tip ingress into the blastocoel (Fig. 1.2E,F). These cells, called secondary mesenchyme cells (SMCs), will give rise to pigment cells, muscle cells, and blastocoelar cells of the larvae. Finally, a pair of coelomic pouches forms from the archenterons via enterocoely (Fig. 1.2 G). A full-grown echinopluteus is bilaterally symmetrical, and typically has 8 or more long, heavily-ciliated feeding arms supported by a calcareous skeleton (Fig. 1.3A). Food particles collected by these ciliated arms are transported to the mouth where they are ingested and enter a tripartite larval gut. Following a period of planktonic existence and larval growth, an echinopluteus will settle on a substrate and undergo metamorphosis to produce a pentamorously-symmetrical juvenile form.

Fig. 1.2. Overview of early development in the echinoid *Dendraster excentricus*. Embryos are oriented with the animal pole up and to the right unless otherwise stated. (A) Four-cell stage with pigmented jelly coat (orientation unclear). (B) Sixteen-cell stage (vegetal view) with micromeres in the foreground (jelly coat still present). (C) Early-blastula stage. (D) Mesenchyme-blastula stage with vegetal plate (vp) and ingressing primary mesenchyme cells (pmc). (E) Early gastrula stage with invaginating archenteron (arc) and ingressing secondary mesenchyme cells (smc). (F) Mid-gastrula stage. (G) Early-prism stage with forming coeloms (co). (H) Early-larva with larval skeleton (sk).
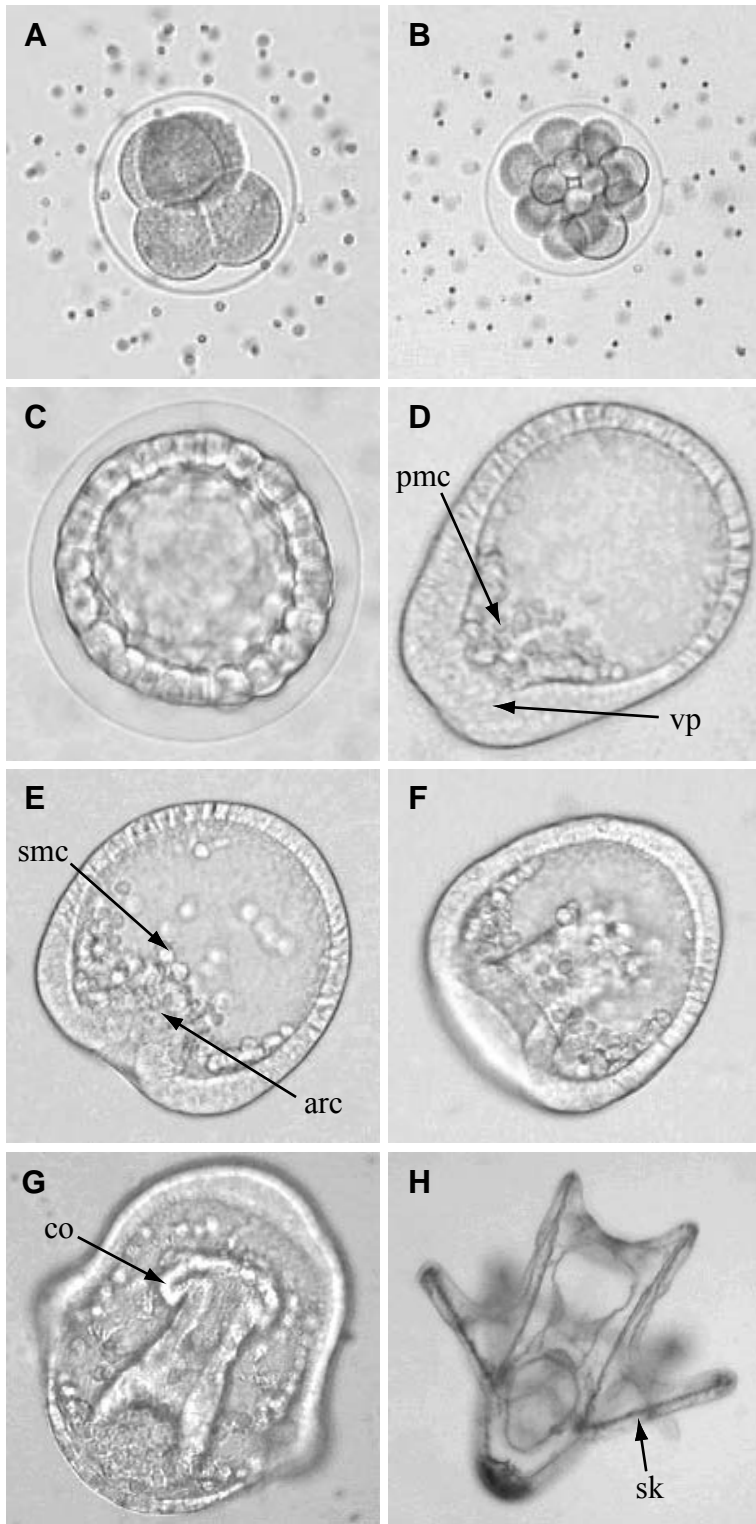
Experimental analysis of echinoid development

Experimental work conducted on sea urchins has broadly defined the mechanisms that underlie embryogenesis and larval developmental in the echinoderm class Echinoidea. Fate maps indicate that ectodermal, endodermal and mesodermal fates are distributed along the animal-vegetal (A-V) axis of the early embryo such that ectodermal fates are at the animal pole and mesodermal fates are at the vegetal pole (Fig. 1.4) (Cameron and Davidson, 1991; Hörstadius, 1973). Isolation and transplantation experiments have shown that proper specification of germ layers is dependent upon a gradient of factors which extend along the A-V axis and a number of intercellular signaling interactions (Hörstadius, 1973). One of the major animalizing factors in the sea urchin embryo (factors involved in ectodermal specification) is SoxB1, which functions by antagonizing vegetalizing factors (Angerer *et al*., 2005; Kenny *et al*., 1999, 2003). Vegetalizing factors (factors involved in endodermal and mesodermal specification) appear to play a more influential role in patterning the early sea urchin embryo and thus have received more attention. One of the earliest and perhaps most important vegetalizing factors in the sea urchin embryo is β-catenin. Several experiments have shown that β-catenin and other components of the canonical Wnt signaling pathway play an instrumental role in the specification of endoderm and mesoderm (Emily-Fenouil *et al*., 1998; Logan *et al*., 1999; Wikramanayake *et al*., 1998). In association with the transcriptional regulators Otx and TFC, β-catenin activates a well-defined
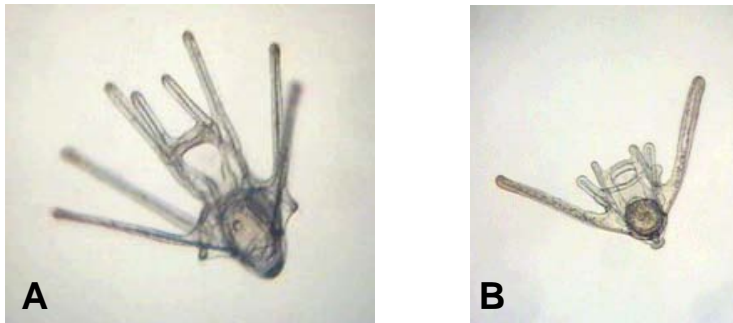
8

Fig. 1.3. Echinoderm pluteus larvae with feeding arms supported by a larval skeleton. (A) An echinopluteus of *Dendraster excentricus*. (B) An ophioputeus of *Ophiopholis aculeata*.

endomesodermal gene network (Davidson *et al.*, 2002; Huang *et al.*, 2000; Li *et al.*, 1999; Vonica *et al.*, 2000).

Intercellular signaling also plays a crucial role in the proper specification of cell fates during sea urchin embryogenesis. Between the 4th and 5th cleavage an inductive signal derived from the micromeres is required for endodermal specification. If the micromeres—which give rise to mesodermal derivatives—are removed before 5th cleavage, embryos with endodermal and mesodermal defects are produced; while these embryos often regulate and produce relatively normal larvae, PMCs are not produced and gastrulation is severely delayed and often incomplete (Ransick and Davidson, 1995). Transplantation of micromeres to the animal pole of a host embryo, on the other hand, results in the induction of an ectopic gut from the presumptive ectodermal host tissue (Ransick and Davidson, 1993). The signaling molecule that mediates this inductive interaction is still unknown. Latter signaling events involved in the specification of secondary mesenchyme cells (pigment and blastocoelar cells) and positioning of the endoderm-ectoderm boundary are mediated by the Notch-Delta signaling system and are endomesodermally-derived (Sherwood and McClay, 1999, 2001; Sweet and Ettensohn, 1999, 2002).

Specification of the dorsal-ventral (D-V) axis has also been examined in sea urchins, although much less is known about this process than A-V specification. Morphological signs of a secondary embryonic axis (i.e. the D-V axis) are not seen in sea urchin embryos until the gastrula stage when PMCs cluster in two vegetal-ventral patches and the oral ectoderm begins to flatten. D-V asymmetries in respiratory activity and
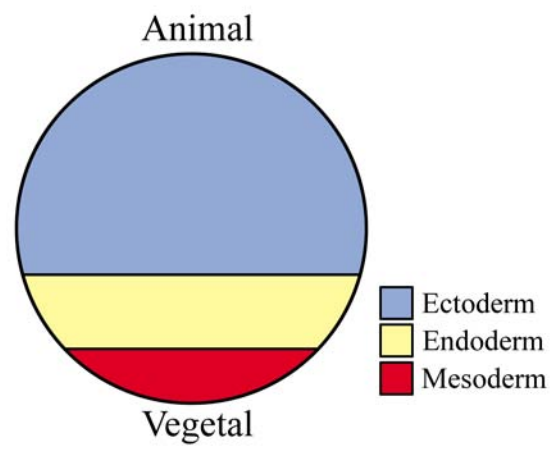
Fig. 1.4. Schematic illustrating the distribution of presumptive larval fates in an echinoid egg. The animal axis (top) marks the site where the polar bodies will be given off.

mitochondrial distribution can be seen in oocytes, however, and these factors are good

predictors of the D-V axis in both unperturbed and experimentally altered embryos

(Coffman and Davidson, 2001; Coffman *et al.*, 2004). Other experiments examining

when the D-V axis is established have yielded contradictory results and interpretations.

Although some lines of evidence suggest that the D-V axis is specified prior to first

cleavage (Cameron *et al.*, 1989; Hörstadius, 1973), other data suggest that this axis can

be perturbed and in some cases reversed through late-cleavage stages (Driesch, 1892;

Hörstadius, 1973). Together these data indicate that while the D-V axis may be specified

in the oocyte, this axis may not be committed until a later cleavage stage. Very little is

known about what molecules are involved in the specification of this axis, although

goosecoid, BMP2/4, Nodal and Activin have recently been implicated (Angerer *et al.*,

2000, 2001; Duboc *et al.*, 2004; Flowers *et al.*, 2004).

Investigating embryogenesis in an ophiuroid

Despite the wealth of knowledge regarding the mechanisms of early development

in echinoids, very little is known about the mechanisms which underlie embryogenesis in

the other groups of the echinoderm-hemichordate clade. Asteroids and enteropneust

hemichordates have received some attention; for these groups, fate maps have been

constructed, some experimental work has been conducted, and expression patterns for a

limited number of genes have been produced. What is known about the development of

the three remaining extant echinoderms is purely descriptive in nature, and therefore

limited in scope. One possibility is that different extant echinoderm classes have evolved

different mechanisms of regional specification. Conversely, it is possible that each of the extant echinoderm classes undergo regional specification the same way. It seems quite possible that the mechanisms that underlie development in echinoids may be quite different from those that function in the other extant classes for two reasons: 1) most echinoids have a modified cleavage pattern in which small micromeres are produced at the 16-cell stage. These micromeres, which are not present in the embryos of other extant classes, play a key role in the process of regional specification in this group. 2) The fossil record indicates that the echinoids went through a bottleneck during the Permian extinction where only one or two genera survived (Erwin, 1993). Extant echinoid genera are therefore the product of a post-Permian radiation and may represent only a limited subset of the developmental patterns that existed prior to the Permian.

The purpose of the research presented here is to determine whether the mechanisms which underlie regional specification in the ophiuroid are similar to or different from those which operate in echinoids, asteroids, and hemichordates. An ophiuroid was chosen for this study primarily because many ophiuroids, like many echinoids, develop indirectly via the production of a pluteus larva (Fig. 1.3); no holothuroids, crinoids, or asteroids develop via a pluteus larva (Fig. 1.1A). Moreover, cladistic analyses indicate that the pluteus larva may have arisen independently in these two classes through a process of convergent evolution (Littlewood *et al.*, 1997; Smith, 1988). It is not known whether these two groups employ similar or divergent developmental mechanisms to construct a pluteus larva.

Several aspects of embryogenesis and larval development were examined in the ophiuroid *Ophiopholis aculeata*. First, embryogenesis was reexamined on a descriptive level. Next, a fate map was constructed of the early embryo through the 8-cell stage. In addition, a series of experiments were performed to examine the distribution of developmental potential in the early embryo. Finally, several attempts were made to uncover mechanisms involved in the specification of embryonic germ layers and the larval dorsal-ventral axis.

Chapter 2: Distribution of larval fates and developmental potential in the early embryo of the brittle star *Ophiopholis aculeata*[*]

Introduction

The phylum Echinodermata is composed of five extant classes—Echinoidea, Holothuroidea, Asteroidea, Ophiuroidea, and Crinoidea—and is a sister-group to the phylum Hemichordata (Hyman, 1955; Cameron *et al*., 2000). Many echinoderm and hemichordate species develop indirectly via free-swimming planktonic larvae (Fig. 2.1). Experimental work conducted on sea urchins has broadly defined the mechanisms that underlie embryogenesis and larval developmental in the echinoderm class Echinoidea (Hörstadius, 1973). Recent investigations have built upon this knowledge by uncovering many of the molecular mechanisms that underlie early development in echinoids. This work has led to the identification of several intracellular signaling pathways, cell-cell interactions and gene regulatory networks known to play fundamental roles in echinoid embryogenesis (for reviews see Ettensohn and Sweet, 2000; Davidson *et al*., 2002; Angerer and Angerer, 2003). Despite the wealth of knowledge regarding the mechanisms of early development in echinoids, very little is known about the mechanisms which underlie embryogenesis in other groups of the echinoderm-hemichordate clade. Much of

what is known about embryonic mechanisms in these other groups is from work examining blastomere fates and the distribution of developmental potential in early asteroid and hemichordate embryos.

The larval fates of blastomeres have been examined in a number of species within the echinoderm-hemichordate clade. Fate-mapping analyses have been conducted on the embryos of multiple echinoid species (Cameron and Davidson, 1991; Cameron *et al.*, 1987; Hörstadius, 1973; Wray and Raff, 1990; Henry *et al.*, 1992), one asteroid species (Kominami, 1983), and two hemichordate species (Colwin and Colwin, 1951; Henry *et al.*, 2001). Comparative analyses of these fate maps indicate that some cell lineage-specific features are variable between taxa; the orientation of the first embryonic cleavage plane with respect to the plane of larval bilateral symmetry is one such feature. These analyses also suggest that other cell lineage-specific features appear to have been highly conserved throughout the evolution of the clade (Raff, 1999). Conserved features include the distribution of larval cell fates along the animal-vegetal axis (A-V axis) and the orientation of the first three embryonic cleavage planes with respect to the A-V axis.

The distribution of developmental potential has also been examined in the echinoderm-hemichordate clade. If blastomeres are separated at the 2-cell stage in the indirect-developing echinoid *Paracentrotus lividis* or the asteroid *Asterina pectinifera*, both blastomeres are capable of producing a small but normal larva (Dan-Sohkawa and Satoh, 1978; Hörstadius, 1973). Similar experiments in the hemichordates *Saccoglossus kowalevskii* and *Ptychodera flava* are consistent with these results (Colwin and Colwin, 1950; Henry *et al.*, 2001), indicating that in these three taxa the potential to form

16
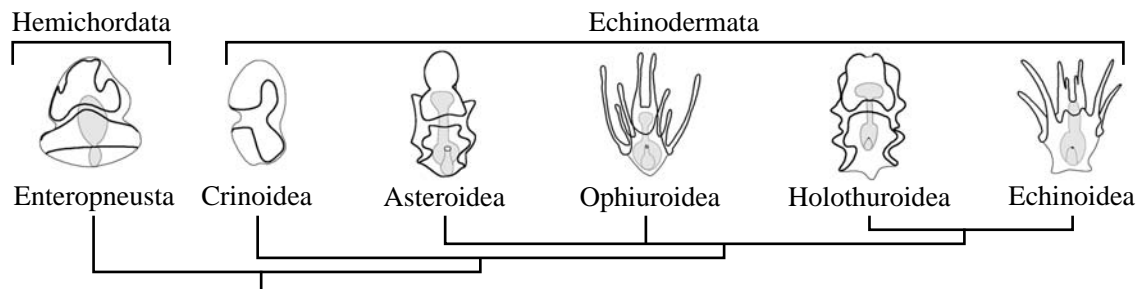
Fig. 2.1. Larval forms of extant echinoderm classes with an enteropneust hemichordate out-group. Crinoids represent the most basal extant echinoderms and echinoids and holothuroids are sister-taxa; placement of asteroids and ophiuroids within this group is less certain. Echinoids and ophiuroids are the only groups which develop via the production of a pluteus larva (which bear long ciliated arms supported by a larval skeleton). This and all ensuing phylogenies are based on Littlewood *et al*., (1997) and Cameron *et al*., (2000).

ectoderm, endoderm, and mesoderm segregates equally into both daughter cells at first cleavage. If the same experiment is conducted in the direct-developing echinoid *Heliocidaris erythrogramma*, on the other hand, one isolate gives rise to more endodermal and mesodermal derivatives than the other, indicating that the potential to form endoderm and mesoderm segregates unequally at first cleavage in this embryo (Henry and Raff, 1990).

If blastomeres are separated along the third cleavage plane at the 8-cell stage in the echinoids *P. lividis* or *H. erythrogramma* or in the asteroid *A. pectinifera*, the vegetal half develops into a small but normal larva while the animal half produces an ectodermal vesicle (Henry and Raff, 1990; Hörstadius, 1973; Maruyama and Shinoda, 1990). These results indicate that while the potential to form ectoderm is present in both the animal and vegetal halves of the embryo at the 8-cell stage, the potential to form endoderm and mesoderm segregate exclusively to the vegetal half of the embryo at third cleavage in these species. These isolation experiments suggest that the distribution of developmental potential has also been highly conserved throughout the evolution of the echinoderm-hemichordate clade; the only exception may be a consequence of a switch in developmental mode. Without the appropriate data from the ophiuroids, holothuroids and crinoids, however, it is difficult to draw any firm conclusions on the matter.

The purpose of this study was to determine whether the mechanisms which underlie regional specification in the ophiuroid *O. aculeata* are similar to or different from those which take place in echinoids, asteroids, and hemichordates. An ophiuroid was chosen for this study primarily because many ophiuroids, like many echinoids,

18

develop indirectly via the production of a pluteus larva; no holothuroids, crinoids, or asteroids develop via a pluteus larva (Fig. 2.1). Moreover, cladistic analyses indicate that the pluteus larva may have arisen independently in these two classes through a process of convergent evolution (Littlewood *et al*., 1997; Smith, 1988). It is not known, however, whether these two groups employ similar or divergent developmental mechanisms to construct a pluteus larva. Therefore, the embryonic axial properties and orientation of early cleavage planes were examined, a fate map of the early embryo was constructed, and a series of experiments were performed on the early *O. aculeata* embryo to elucidate the mechanisms which underlie the process of regional specification in this embryo. This work represents the first piece of experimental embryology conducted on any member of the echinoderm class Ophiuroidea.

Materials and methods

Animals and embryos

  Ophiopholis aculeata adults were collected intertidally on San Juan Island, WA, and were maintained at 10-12˚ C in aquaria with running sea water. To induce spawning, animals were exposed to a combination of bright light, heat and physical perturbation (shaking, swirling and/or inversion) for 1-2 hours. Animals were then placed in filtered sea water (FSW) at 12˚ C in individual bowls; spawning took place within the next few hours. Spawned oocytes were rinsed several times in FSW and fertilized with a dilute sperm concentration. Following fertilization, these embryos were rinsed several times

and raised in pasteurized Jamarin artificial sea water (JSW; Jamarin Labs, Osaka, Japan).

Spawned oocytes to be used for blastomere separation experiments were fertilized in

FSW containing 10 mM para-aminobenzoic acid (PABA, Sigma), which prevents

hardening of the fertilization envelope. Following fertilization, these embryos were

rinsed several times in both FSW containing 10mM PABA and JSW. Embryos were

subsequently pipetted up and down in a small-bore pipette to remove fertilization

envelopes. Prior to histochemical analysis, larvae were fixed overnight in 4%

paraformaldehyde in JSW.

Propidium iodide and phallacidin staining

Because *O. aculeata* embryos are opaque, fluorescent dyes and confocal imaging

were used to make cytological observations. The fluorescent dyes used include

propidium iodide (Sigma) and BIODIPY FL phallacidin (Molecular Probes), which are

nucleic acid-specific and filamentous actin-specific, respectively. Fixed embryos were

rinsed in phosphate-buffered saline with 0.1% Triton X-100 (PBT), incubated in a PBT

solution with 10 µg/ml propidium iodide and/or 5 units/ml phallacidin, rinsed, dehydrated

and cleared in benzyl benzoate and benzyl alcohol (2:1). Stained samples were imaged

with a BioRad Radiance 2000 laser-scanning confocal microscope.

Cleavage plane orientation analysis

To analyze the orientation of the first two cleavage planes in *O. aculeata,*

embryos fixed just before or after first or second cleavage were stained with propidium

iodide and imaged with a confocal microscope. Embryonic material was treated with extreme care in these cases so as not to disrupt the positioning of polar bodies. Only one measurement was made per embryo (on the position of either the first or second cleavage plane). Confocal z-series stacks were geometrically transformed with ImageJ and the TransformJ plugin so that the polar bodies and two daughter nuclei of the cleavage of interest were in the same focal plane. The angle between the polar bodies (which mark the animal pole) and the cleavage plane of interest (defined by either the cleavage plane itself, an initiating cleavage furrow, or a line equally bisecting segregating mitotic chromosomes) was then measured using ImageJ.

Lineage-tracer injections and cell fate analysis

Microinjections were performed in a Kiehart injection chamber (Kiehart, 1982). Embryos were incubated in a calcium-free, magnesium-depleted artificial sea water solution (394.5mM NaCl, 12.21mM $MgCl_2$, 27.56mM Na_2SO_4, 8.63mM KCl, 2.3mM $NaHCO_3$, 10mM Tris, 2.5mM disodium EGTA pH 8.0) shortly before and during the injection period to soften the hyaline layer of the embryos. Individual blastomeres were pressure-injected with a 1:1 mixture of 50 mg/ml 10,000MW rhodamine-labeled dextran and biotinylated dextran (Molecular Probes) in a 0.2M KCl solution. Following injection, embryos were returned to JSW and raised either alone or with a few siblings. Injected embryos were viewed regularly with a dissecting scope equipped with epifluorescence, and abnormal embryos were discarded. Embryos were imaged between 2-12 days post-fertilization with a confocal microscope (as above) and/or with Nomarski

optics following visualization of biotinylated-dextran. Biotinylated-dextran was visualized by a streptavidin-horseradish peroxidase and diaminobenzadine staining procedure as described in Freeman and Martindale (2002), except that following the DAB reaction and rinses with PBS-Triton, larvae were immediately dehydrated and cleared in benzyl benzoate and benzyl alcohol (2:1). Several injected larvae were imaged at two or more developmental stages.

Operative methods

Blastomere isolation experiments were conducted at the 2-, 4- and 8-cell stages in JSW on a substrate of 2% agar dissolved in JSW. Fertilization envelops were removed prior to first cleavage as described above. To separate blastomeres, or sets of blastomeres, a microfilament loop was tightened around the cleavage plane of interest as described in Freeman (1993). Following operations, embryos were raised individually and monitored regularly. At 6-7 days post-fertilization, larvae were assayed for the presence of spicules using a compound scope equipped with polarizing optics, and many larvae were assayed for the presence of gut tissue with a non-specific alkaline phosphatase reaction. To identify the second cleavage plane at the 4-cell stage, one blastomere was marked laterally at the 2-cell stage using Nile blue and second cleavage was observed. In all other cases, Nile blue marks were made at either the animal or vegetal pole just after polar body formation; the site of polar body expulsion defined the animal pole. Identification of the third cleavage plane at the 8-cell stage was based on an observation of that cleavage and the position of the polar bodies or the position of a Nile

blue mark made on the zygote. In a number of cases, Nile blue marks were used to indicate the embryonic origin of isolates produced at either the 2- or 8-cell stage. Nile blue marks were applied by bringing the tip of a staining micropipette in contact with an embryo for 10-20 seconds using a Singer micromanipulator. Staining micropipettes were filled with the vital dye Nile blue A in agar and pulled to a fine tip. Nile blue marks persist for at least 4 days and embryos develop normally if not over-stained.

Alkaline phosphatase histochemistry

Samples were tested for the localization of alkaline phasphatase using a modification of an indoxyl-tetrazolium procedure developed by McGadey (1970). Recipes for the solutions used here are from Whittaker and Meedel (1989). Following a 1-2 hour staining period, materials were dehydrated and cleared in benzyl benzoate and benzyl alcohol (2:1).

Results

Embryogenesis and larval development

Embryogenesis and larval development in *O. aculeata* have been previously described (Olsen, 1942). This description is supplemented here with the results of a more detailed investigation of several embryonic features. Comparison of these processes with those of a typical indirect-developing sea urchin (class Echinoidea), indicates that while many developmental features between the two groups are similar, several of these features differ significantly.

O. *aculeata* oocytes average 100-105μm in diameter when shed. Polar bodies are produced between 30-60 minutes after spawning occurs in both fertilized and unfertilized eggs. In most cases two polar bodies are produced within 5 μm of each other. The first three embryonic cleavages in *O. aculeata* are equal (Fig. 2.2A-E).   In most sea urchins, the fourth cleavage is equal in the animal blastomeres but unequal in the vegetal blastomeres. The unequal cleavages that occur in the 4 vegetal blastomeres give rise to 4 large macromeres on top of 4 small micromeres. The progeny of these micromeres divide more slowly than non-micromere lineages (Endo, 1966).   In contrast, all cells of the *O. aculeata* embryo divide equally at fourth cleavage and do not make micromeres or macromeres (Fig. 2.2F). Moreover, observations of live and phallacidin/propidium iodide-stained embryos indicate that cell divisions do not become asynchronous in any cell lineage of the *O. aculeata* embryo through the 64-cell stage (data not shown).

Cleavage in *O. aculeata* also differs from that of a normal sea urchin with regard to the spatial arrangement of blastomeres in early cleavage stage embryos. Rather than being organized in orderly tiers as is the case in sea urchins, early cleavage-stage embryos are typically arranged in a more compact manner. In these embryos, blastomeres are pushed between each other, so as to occupy the least amount of space (Olsen, 1942; personal observation). For example, rather than forming a 4-cell stage in which all 4 blastomeres rest on a flat surface, ~70-80% of 4-cell stage *O. aculeata* embryos form a tetrahedral stage. In this tetrahedral stage, the second cleavage plane produced by one blastomere at the 2-cell stage is often perpendicular to the second cleavage plane produced by the other blastomere of the 2-cell stage (Fig. 2.2B, 2.5B).

The arrangement of blastomeres in the remainder of 4-cell stage embryos more closely resembles those of a sea urchin (Fig. 2.2B,D). It should be noted that very few embryos show a tetrahedral arrangement if the fertilization envelope has been removed prior to the 4-cell stage; in these cases, many embryos show a blastomere arrangement intermediate to the two described above.

Following a period of early cleavage, the *O. aculeata* embryo forms a hollow blastula, the vegetal end of which flattens to form a vegetal plate. Prior to the onset of gastrulation, cells within the vegetal plate ingress into the blastocoel (Fig. 2.2G,H). Following invagination, mesenchyme cells continue to be produced but are now derived from the elongating archenteron. During gastrulation, numerous mesenchyme cells become localized in two lateral clusters and produce tri-radiate calcareous spicules that ultimately become the larval skeleton (Fig. 2.2H,I). Experiments in which Nile blue marks were made either at the animal (n=10) or vegetal pole (n=9) of the zygote just after polar body expulsion confirmed that the vegetal pole of the embryo is the site of vegetal plate formation and archenteron invagination (Fig. 2.3A,B). These experiments also indicate that the site of gastrulation ultimately becomes the anus of the larva. Coelom formation is enterocoelous and takes place near the end of gastrulation at the tip of the elongating archenteron. By the fourth day of development, a pluteus larva with a tripartite gut, arms supported by calcareous spicules, and an oral field with a well defined ciliated band has formed. At a morphological level, the features of *O. aculeata* development closely resemble those involved in the development of typical sea urchin larvae. The rates of larval development in *O. aculeata* and the irregular echinoid

25

Fig. 2.2. Embryogenesis and larval development in *O. aculeata*. (A) 2-cell stage; animal pole is up. (B,C) 4-cell stages. Schematics of blastomere arrangements are presented as inserts. (B) Tetrahedral arrangement. Broken-lines indicate cell boundaries located behind blastomeres in a more-proximal focal plane. (C) Non-tetrahedral arrangement. (D) 8-cell stage. (E) 16-cell stage. (F) Mesenchyme blastula stage; anterior is upper-left. (G) Confocal section of mesenchyme-blastula stage stained with propidium iodide; anterior is up. Mesenchyme cells (arrow) have already begun to ingress from the vegetal plate (arrowheads). (H,I) Anterior is upper-left. (H) Late-gastrula stage. Two lateral clusters of skeletogenic mesenchyme cells are present (arrows). The blastopore (arrowhead) has formed within the vegetal plate. (I) 4-day ophiopluteus larva. Scale bars 25μm in A-H; 100μm in I.
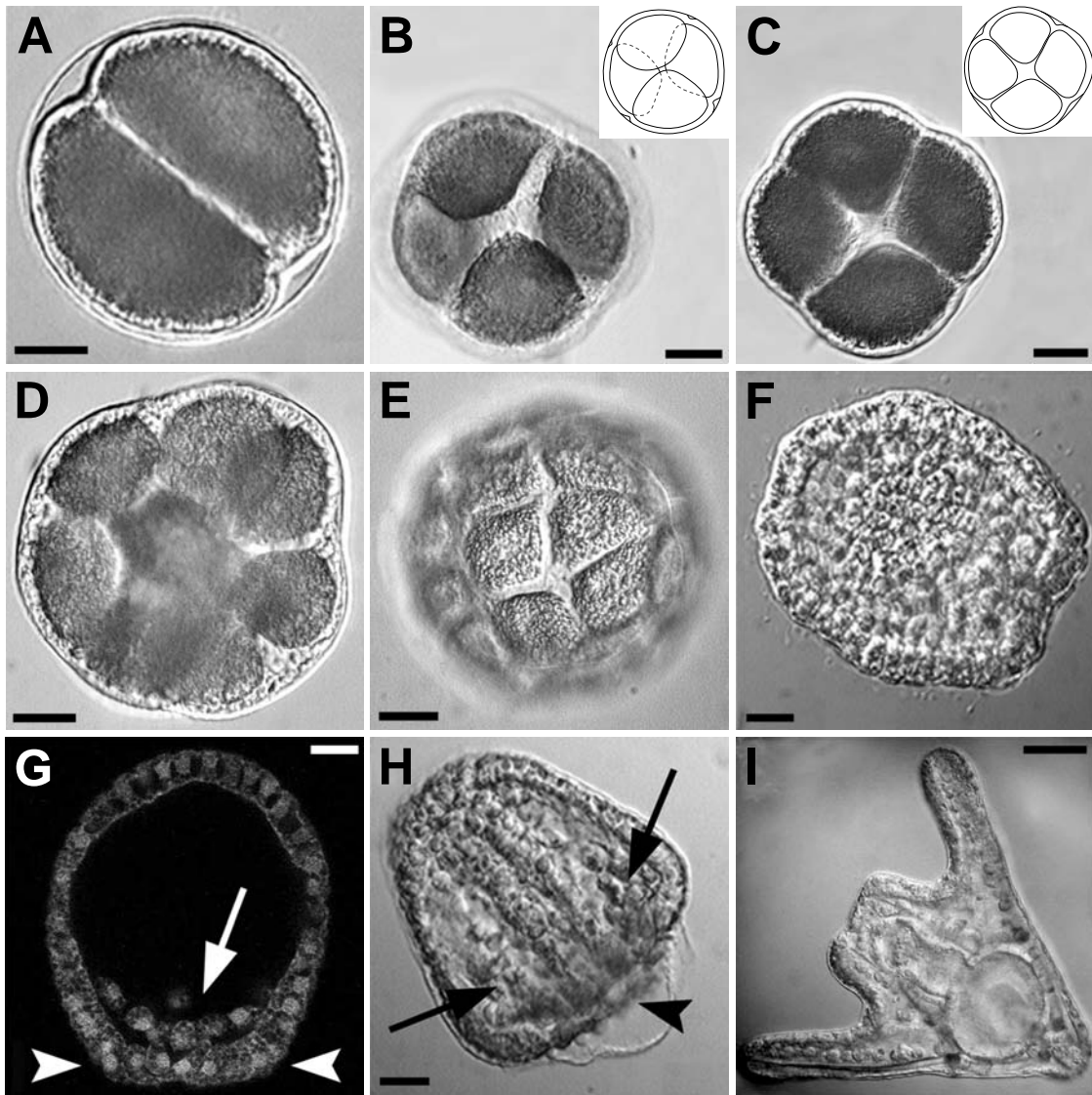
Dendraster excentricus, with eggs of ~115µm in diameter, are similar. In *O. aculeata*, fourth cleavage occurs at 6 hours post-fertilization (hpf), hatching occurs between 17-19hpf, mesenchyme cell ingression begins between 22-28hpf, gastrulation is initiated between 27-30hpf, spiculogenesis begins between 36-38hpf and the first two larval arms begin to form between 60-65hpf. In *D. excentricus* these same events occur at 5 hours and 15 minutes post-fertilization, 17-19hpf, 24-26hpf, 28-29hpf, 30-31hpf, and 55-60hpf, respectively.

Multiple, often overlapping designations have been used to describe the different regions of echinoderm embryos and larvae (for examples, see Davidson *et al*., 1998; Hörstadius, 1973; Kühn, 1971). The designations used here will most closely follow those used by Olsen, (1942) and Hörstadius, (1973). Specifically, the ophiopluteus has three larval axes: an anterior-posterior (A-P) axis, a dorsal-ventral (D-V) axis, and a right-left (R-L) axis (Fig. 2.4). The A-P and D-V axes run parallel to the plane of bilateral symmetry; the R-L axis runs perpendicular to this plane. The A-P axis intersects the mouth (at the more anterior end) and the spot where the right and left spicules converge (at the more posterior end). The larva swims along its A-P axis, leading with its anterior end. The ophiopluteus is much thinner along its D-V axis than it is long or wide along its A-P or R-L axes, respectively. Consequently, the most prominent surfaces of the larva are its dorsal and ventral surfaces. These surfaces are bounded by the larva's leading and trailing edges. The ventral surface includes the mouth, anus, ciliated-band, oral ectoderm and aboral-ectoderm (Fig. 2.4). The dorsal surface contains mostly aboral-ectoderm, but also contains ciliated band along the anterior edge.
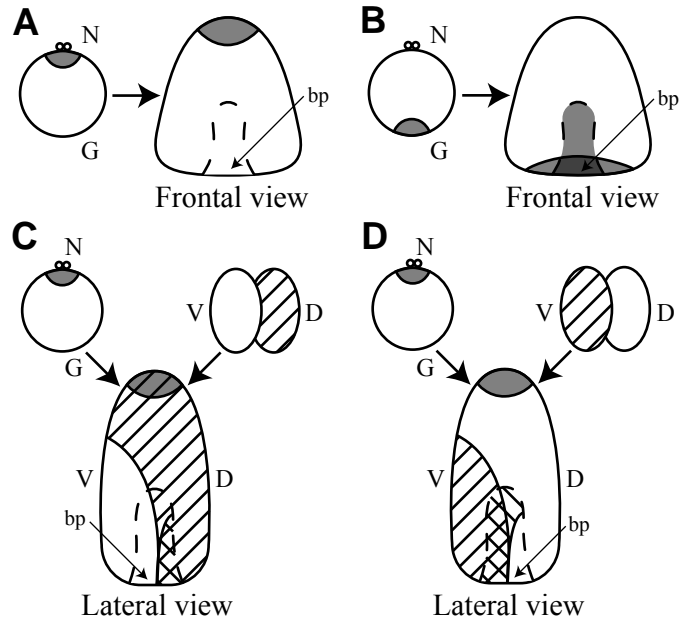
Fig. 2.3. Axial properties of *O. aculeata* embryos and their relation to the first cleavage plane. Nile blue marks represented by grey shading. Injected lineage-tracer dye represented by diagonal lines. The small circles atop zygotes represent polar bodies (N, animal; G, vegetal; D, dorsal; V, ventral; bp, blastopore). The posterior pole of gastrulae is coincident with the blastopore. (A,B) Nile blue marks made at the animal (A) or vegetal (B) pole of a zygote just after polar body expulsion indicate axial properties mid-gastrula stage embryos. (C,D) Superimposition of labeling patterns created by lineage-tracer injection into either the dorsal-(C) or ventral-blastomere (D) at the two cell stage on mid-gastrula stage embryos that had been marked at the animal pole as a zygote (as in A). Mesenchyme cells are typically labeled by the lineage-tracer in D but not C.

Orientation of early cleavage planes with respect to the A-V axis

In echinoids, the first two cleavage planes are meridional (i.e. they intersect the A-V axis of the embryo), and the third cleavage plane is equatorial (i.e. it is perpendicular to the A-V axis) (Boveri, 1901). In the original description of *O. aculeata* development, the only information that was given regarding the orientation of early embryonic cleavage planes was presented in a hand-drawn figure (Olsen, 1942). This figure shows a 2-cell embryo in which the first cleavage plane does not intersect the polar bodies (which mark the animal pole). While this suggested that the first cleavage plane may not coincide with the A-V axis of the embryo, the situation was left uncertain. To address this matter more definitively, the orientations of the first two embryonic cleavage planes in *O. aculeata* were examined more closely by measuring the distance between each cleavage plane and the location of the polar bodies (which should mark the animal pole and define the A-V axis of the embryo). Although rare, cases in which polar bodies were separated by more than 5 μm were excluded from the following analysis. The distance between the first cleavage plane and the position of the polar bodies ranged from 25-65° with a mean of approximately 45° and a standard deviation of less than 11° (n=24; Fig. 2.5A,C). In analyses of the second cleavage plane, distance was measured between the polar bodies and the cleavage plane that formed in the blastomere of 2-cell stage which was adjacent to the polar bodies (the more animal blastomere). This distance ranged from 36-68° with a mean of approximately 45° and a standard deviation of less than 8° (n=20; Fig. 2.5B,D). These results indicate that neither the first nor the more animal of the two second
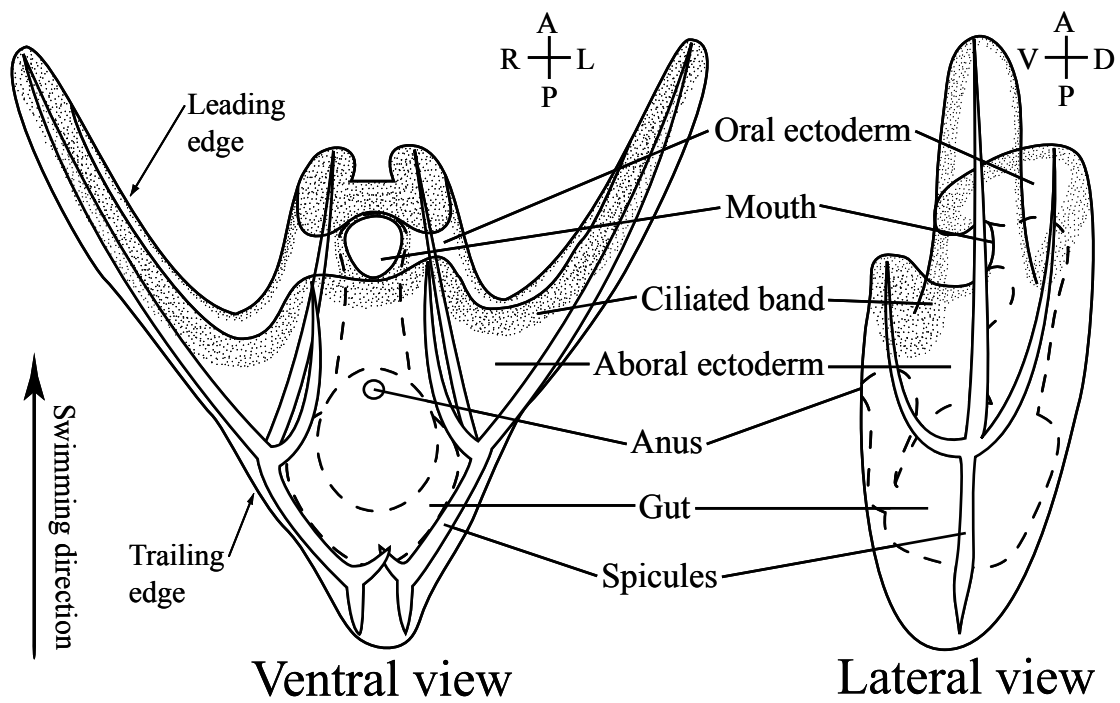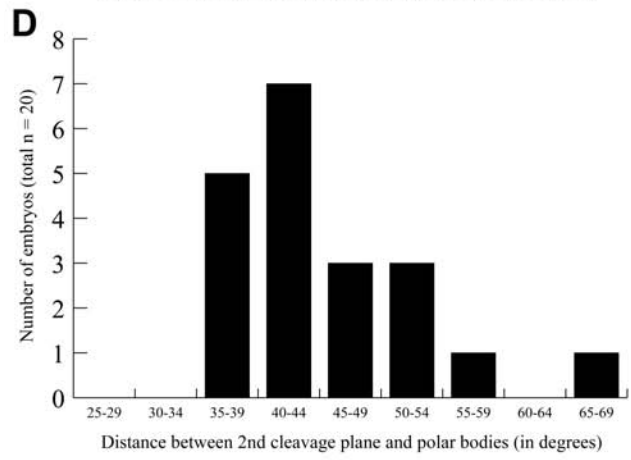
Fig. 2.4. Schematic of 7-day ophiopluteus from both a ventral and lateral view. Stippled regions indicate the ciliated-band and broken lines indicate the gut. Larval axes are indicated for each larva (A, anterior; P, posterior; R, right; L, left; V, ventral; D, dorsal).

Fig. 2.5. Orientation of the first two cleavage planes with respect to the A-V axis. (A,B) Projections of confocal stacks illustrating propidium-iodide stained embryos just after first (A) and second (B) cleavage. Stained polar bodies can be seen at the tops of both images. (A) 2-cell stage. (B) 4-cell stage (tetrahedral arrangement). Second cleavage plane bisecting blastomeres derived from the more animal blastomere at 2-cell stage is indicated with an arrow; second cleavage plane bisecting the other blastomeres is coincident with plane of page. (C,D) Distribution of degrees measured between the polar bodies and the first (C) and second (D) cleavage plane. Scale bar 25µm.

C

Distance between 1st cleavage plane and polar bodies (in degrees)

D

Distance between 2nd cleavage plane and polar bodies (in degrees)
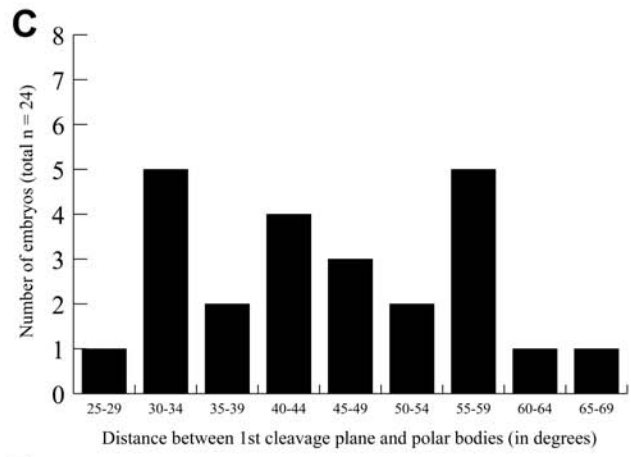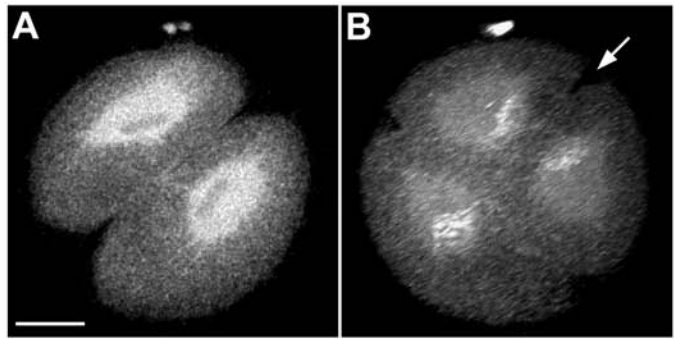
cleavage planes in the *O. aculeata* embryo coincide with the A-V axis of the oocyte. Instead, both cleavage planes are tilted roughly 45º from the A-V axis, as defined by the position of the polar bodies.

Fate map of early embryo

To establish the larval fates of cells that make up the early *O. aculeata* embryo, individual blastomeres were injected with lineage-tracers at the 2-, 4- and 8-cell stages (Table 2.1). Injecting one blastomere at the 2-cell stage produced one of two characteristic distributions of labeled clones. In approximately half of these cases, the injected blastomere gave rise to all of the mesoderm (including skeletogenic mesenchyme and coelomic vesicles), the ventral portion of the ciliated band (termed the ventral ciliated-band ectoderm) and most of the endoderm (Fig. 2.6A,A'). The cell injected in these cases will be designated the ventral blastomere because it gave rise to the ventral ciliated band ectoderm. In the remainder of cases, the injected blastomere gave rise to a small portion of the posterior-most dorsal endoderm and all of the ectoderm excluding the ventral ciliated-band ectoderm (Fig. 2.6B,B'). This cell will be designated the dorsal blastomere and the ectoderm labeled in these cases will be referred to as the non-ventral ciliated-band ectoderm. Superimposing either of these staining patterns as seen at the late-gastrula stage on late-gastrulae which had been marked at the animal pole just after polar body expulsion with Nile blue supports the earlier finding that the first cleavage plane in *O. aculeata* does not intersect the animal pole (Fig., 2.3C,D). These results indicate that the first cleavage plane is perpendicular to the prospective larval D-V axis,

34

Table 2.1
Summary of lineage-tracer injections

Stage Injected	Fates of Injected Ventral Blastomeres			Fates of Injected Dorsal Blastomeres		Total injections	Multistage analysis[a]
	VCB Ectoderm, Endoderm & Mesoderm	Endoderm & Mesoderm	VCB Ectoderm & Endoderm	Non-VCB Ectoderm & Endoderm	Non-VCB Ectoderm		
2-cell	20	-	-	16	-	36	5
4-cell	16	-	-	15	7	38	6
8-cell	7	5	1	4	7	24	5

Note: VCB Ectoderm = ventral-ciliated band ectoderm; Non-VCB Ectoderm = non-ventral-ciliated band ectoderm.
[a] Indicates the number of injected embryos raised individually and documented at multiple time points.

roughly dividing the ectoderm in to a more-dorsal and more-ventral territory; this has previously been referred to as a frontal cleavage plane (Henry and Raff, 1990).

Although the labeled blastomere in each of these cases gave rise to one of two characteristic distribution patterns of labeled clones, the exact location of the boundaries of these labeled clones within the larva was variable between larvae. This variability was most apparent in the posterior larval endoderm. The total amount of endoderm derived from the dorsal blastomere in these injections varied from less than 10% to over 50% (Table 2.2). This variability was limited, however, in that for over 90% of the cases less than 25% of the gut (always the most posterior-dorsal region of the gut) was derived from the dorsal blastomere. These results indicate that while the fates of each blastomere at the 2-cell stage are highly reproducible, the exact fates of these blastomeres are not completely stereotypical.

At the 4-cell stage, in just under half the cases, the injected blastomere gave rise to ventral ciliated band ectoderm, mesoderm and endoderm (Fig. 2.6C,C',D,D'). The injected blastomeres in these cases were daughters of the ventral blastomere. In the remainder of the cases at the 4-cell stage, the injected blastomere either gave rise to non-

Fig. 2.6. Projections of confocal stacks illustrating larvae in which individual blastomeres have been injection-labeled at the 2-, 4-, or 8-cell stage. Red indicates the labeled clones derived from the injected blastomere and green indicates a silhouette of the injected larva. Anterior is to the upper left in all cases (except in K, where the animal pole is up). Each letter pair (for example, A and A'), represent two images of the same larva, each showing a different side of that larva (except in K, K', and K"). (A-J) Ventral views. (A'-J') Dorsal views. (A,B) Injection of a single blastomere at the 2-cell stage. (A,A') Injection of a ventral blastomere. (B,B') Injection of a dorsal blastomere. (C-F,C'-F') Injection of a single blastomere at the 4-cell stage. (C,C') Injection of a left ventral blastomere. (D,D') Injection of a right ventral blastomere. (E,E') Injection of a daughter-cell of a dorsal blastomere (a left dorsal blastomere in this case). (F,F') Injection of a daughter-cell of a dorsal blastomere (a right dorsal blastomere in this case). (G-K,G'-K',K") Injection of a single blastomere at the 8-cell stage. (G,G') Injection of an anterior ventral blastomere. (H,H') Injection of a posterior vegetal blastomere. (I,I') Injection of an anterior dorsal blastomere. (J,J') Injection of a posterior dorsal blastomere. (K,K',K") Injection of an anterior ventral blastomere (imaged at multiple time-points). (K) Late-blastula stage (48 hours). Dorsal view with archenteron extending upwards. Labeled derivatives of injected blastomere make up much of the left side and tip of archenteron, part of the ectoderm located near the blastopore, and some of the mesenchyme which is forming a ring around the archenteron in the vegetal region of the blastocoel. (K',K") Early-larval stage (5 days) of same embryo showing ventral (K') and dorsal (K") views. Injected blastomere results in labeling of ventral ciliary band ectoderm, gut, and mesoderm; note that what is seen on the left in K and K" is shown on the right in K'. Scale bars 100µm. Scale bar in A applies to all images except K.
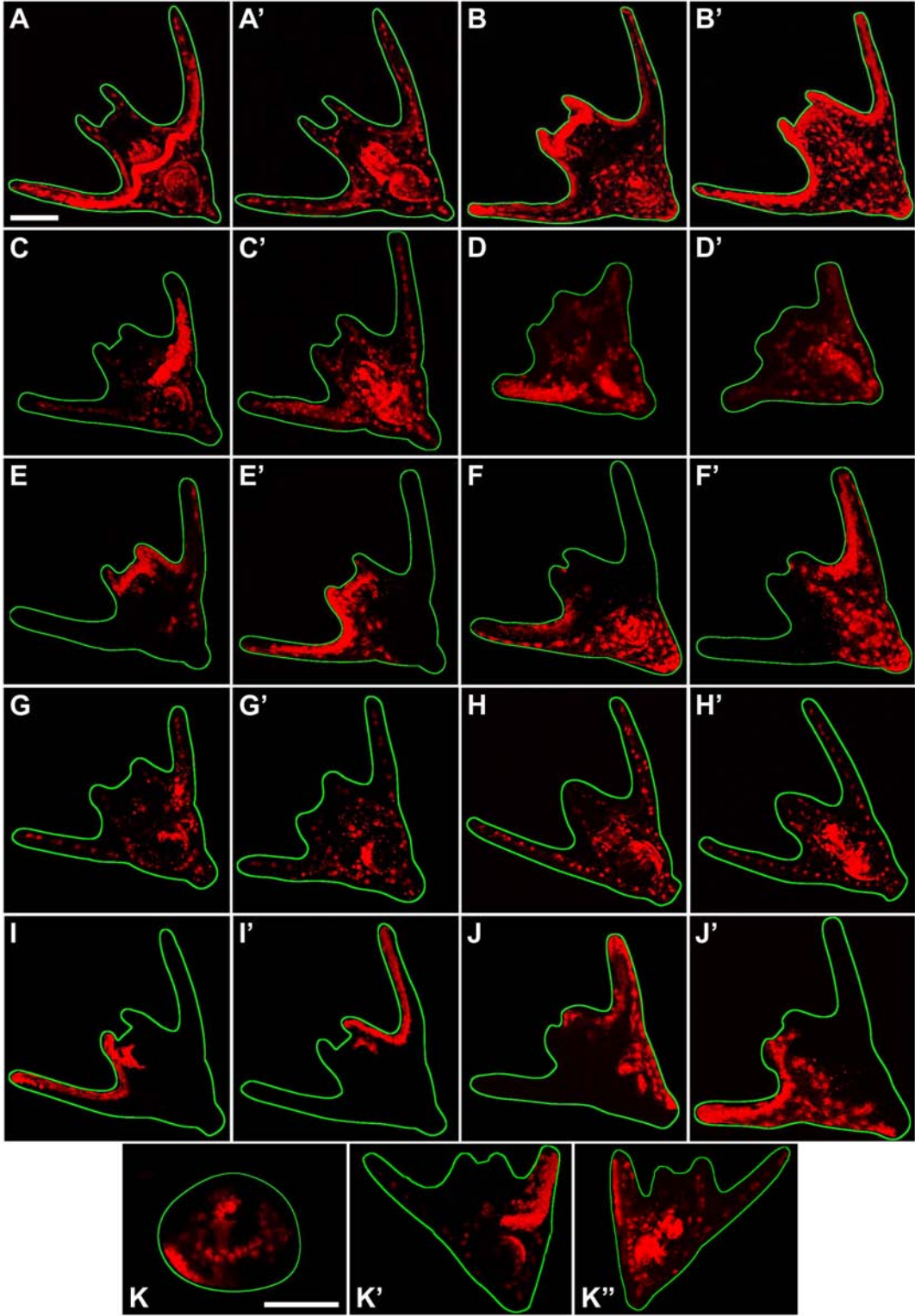
Table 2.2
Summary of variation following single-cell labeling at 2-cell stage

	% endoderm derived from dorsal blastomere			
	$\leq 10\%$	10%-25%	25%-50%	$\geq 50\%$
Number of cases	19 (56%)	12 (35%)	2 (6%)	1 (3%)

Based on cases where either the dorsal or ventral blastomere was injected.
() indicate percentage of total cases.

ventral ciliated band ectoderm (Fig. 2.6E,E'), or both non-ventral ciliated band ectoderm

and posterior dorsal endoderm (Fig. 2.6F,F'). The blastomeres injected in these cases

were daughters of the dorsal blastomere. The fact that the daughters of the dorsal

blastomere gave rise to endoderm in well over half, but not all, of the cases, indicates that

in some embryos both daughters of the dorsal blastomere gave rise to ectoderm and

endoderm, whereas in other embryos one dorsal blastomere-daughter cell gave rise

ectoderm and endoderm and the other gave rise to just ectoderm.

In almost all of the dorsal-daughter blastomere injections at the 4-cell stage in

which the angle of the boundary of labeled ectodermal clones could be clearly established

(n=27), this boundary fell near a plane which is half way between the larval anterior-

posterior axis and the larval right-left axis (Fig. 2.6C-F,C'-F') indicating that the second

plane of cleavage in the dorsal blastomere corresponds to a plane approximately 45º off

the plane of larval bilateral symmetry. These results support our earlier findings that the

second cleavage plane in the more animal blastomere (i.e. the dorsal blastomere) is

approximately 45º off the A-V axis of the embryo, assuming that the larval plane of

bilateral symmetry runs parallel to the A-V axis. In addition, in almost half of these cases

the boundary of labeled ectodermal clones fell 45º clockwise of the larval plane of

bilateral symmetry (n=13; Fig. 2.6E,E',F,F'), and in the remainder of these cases the boundary of labeled ectodermal clones fell 45º counter-clockwise of the larval plane of bilateral symmetry (n=14). Mesenchymal cells labeled from injections at the 4-cell stage were found throughout the larva (Fig. 2.6C,C',D,D'), indicating that mesenchyme derived from one side of the vegetal plate migrates throughout the embryo during development. The number of mesenchyme cells labeled from these injections was well over half of those labeled from injections at the 2-cell stage, indicating that these mesenchymal cells are somehow sharing cytoplasm, perhaps by forming syncytial mesenchymal clusters similar to those known to form in echinoid embryos (Hodor and Ettensohn, 1998). Mesenchymal and endodermal cell migration prevented a more detailed analysis of the axial orientation of ventral-daughter blastomere clonal boundaries.

At the 8-cell stage, in about half the cases the injected blastomere was a descendent of the ventral blastomere. In these cases the labeled blastomere gave rise to ventral-ciliated ectoderm, endoderm, and mesoderm (Fig. 2.6G,G'), ventral ciliated band ectoderm and endoderm (data not shown), or endoderm and mesoderm (Fig. 2.6H,H'). The cases where the non-ventral ciliated band was labeled are thought to be the result of injecting one of the anterior ventral blastomeres and those that lack ectodermal staining are thought to be the result of injecting one of the posterior ventral blastomeres. In the remaining cases at the 8-cell stage, the injected blastomere was a descendent of the dorsal blastomere. These blastomeres gave rise to either anterior non-ventral ciliated band ectoderm (Fig. 2.6I,I') or both posterior non-ventral ciliated band ectoderm and posterior

dorsal endoderm (Fig. 2.6J,J'). Injected blastomeres which gave rise to only ectoderm are thought to have been anterior dorsal blastomeres and those which gave rise to both ectoderm and endoderm are thought to have been posterior dorsal blastomeres. The exact location of the clonal boundaries of injected blastomeres in these cases varied slightly from embryo to embryo.

To ensure that the labeled clones followed normal patterns of development, a number of embryos injected at each stage were raised individually and imaged at multiple time-points during development. These embryos were observed regularly and typically imaged at both a late-gastrula and larval stage (Fig. 2.6K,K',K"). In each of these cases, the patterns of development of labeled clones was consistent with expectations based on normal development (i.e. labeled archenteron always gave rise to labeled endoderm, labeled ectoderm always gave rise to appropriately positioned labeled epidermis, etc.). These results are summarized in Fig. 2.7A,B. Because the second cleavage plane appears to lie 45° clockwise or counterclockwise from the line of larval bilateral symmetry (depending on the embryo), larval fates are most likely not distributed symmetrically across the second cleavage plane as indicated in Fig. 2.7. Rather than presenting two different fate maps (one with endomesodermal fates biased to the right and one with endomesoderm biased to the left), only one schematic fate map is presented for simplicity.

Distribution of developmental potential in the early embryo

To establish the distribution of developmental potential in the early *O. aculeata* embryo, cleavage-stage embryos were separated along one of the first three cleavage planes. First, embryonic fragments were separated along the first cleavage plane at the 2-cell stage. In 27 cases, both isolates were still alive at the time of analysis (Table 2.3). In the majority of these cases (n=20), both blastomeres gastrulated and gave rise to ectodermal, endodermal, and mesodermal derivatives. In all of these cases, however, although one member of the pair formed a small but phenotypically normal pluteus larva with appropriate amounts of ectodermal, endodermal, and mesodermal derivatives, the other formed a small, abnormal pluteus with a disproportionately-small gut and a reduced larval skeleton (Fig. 2.8A,A'). Moreover, the timing of gut and skeleton formation in these cases was delayed. In the remaining cases (n=7), one blastomere gastrulated and gave rise to a small but phenotypically-normal larva and the other did not gastrulate and gave rise to a hollow, ciliated ectodermal vesicle lacking mesodermally-derived skeletogenic mesenchyme and endodermally-derived gut tissue (Fig. 2.8B,B').

In 12 of the above cases, one of the blastomeres was marked with Nile blue at the 2-cell stage (based on the position of the polar bodies) so that the embryonic origin (i.e. more animal half or more vegetal half) of the isolates could be identified at the time of analysis. In each of these cases the more vegetally derived isolate gave rise to more endoderm and mesoderm, regardless of whether the mark was made on the more animal (n=6) or more vegetal half (n=6) of the embryo.

41

Fig. 2.7. Summary of fate-mapping studies with comparison to the fate maps of other echinoderms and hemichordates. Color-coded legend in A applies to B-D as well. (A) 8-cell fate map of *O. aculeata* with the first cleavage plane vertical and perpendicular to the plane of the page, the second cleavage plane coincident with the plane of the page and the third cleavage plane horizontal and perpendicular to the plane of the page; cleavage plane orientations are the same for echinoid, asteroid and hemichordate embryos in (D). Although this schematic accurately represents individual blastomere fates, blastomere-pairs separated by the second cleavage plane may not contain equal amounts of specified germ layer derivatives as indicated due to skewed second cleavage plane; the same is true for (D). (B,C) Cell-lineages through the 8-cell stage with germ layer-specific contributions of each lineage indicated for *O. aculeata* (B) and a typical echinoid, asteroid or hemichordate (C). Indicators of blastomere lineage based on Cameron *et al.* (1987) and Wray and Raff (1989), (D, dorsal: V, ventral; L, lateral; N, animal; G, vegetal; A, aboral; O, oral). (D) Fate map of *O. aculeata* embryo at the 8-cell stage compared to that of echinoids, hemichordates and an asteroid. Echinoid, asteroid and hemichordate fate-maps based on Cameron *et al.*, (1987), Wray and Raff, (1989), Kominami, (1983), Henry *et al.*, (2001), and Colwin and Colwin, (1951), respectively.

42

A

Ectoderm
Endoderm
Mesoderm

B

C

D

Echinoid
(Indirect-developer)

Strongylocentrotus purpuratus

Echinoid
(Direct-developer)

Heliocidaris erythrogramma

Asteroid

Asterina pectinifera

Ophiuroid

Ophiopholis aculeata

Hemichordates

Ptychodera flava, Saccoglossus kowalevskii

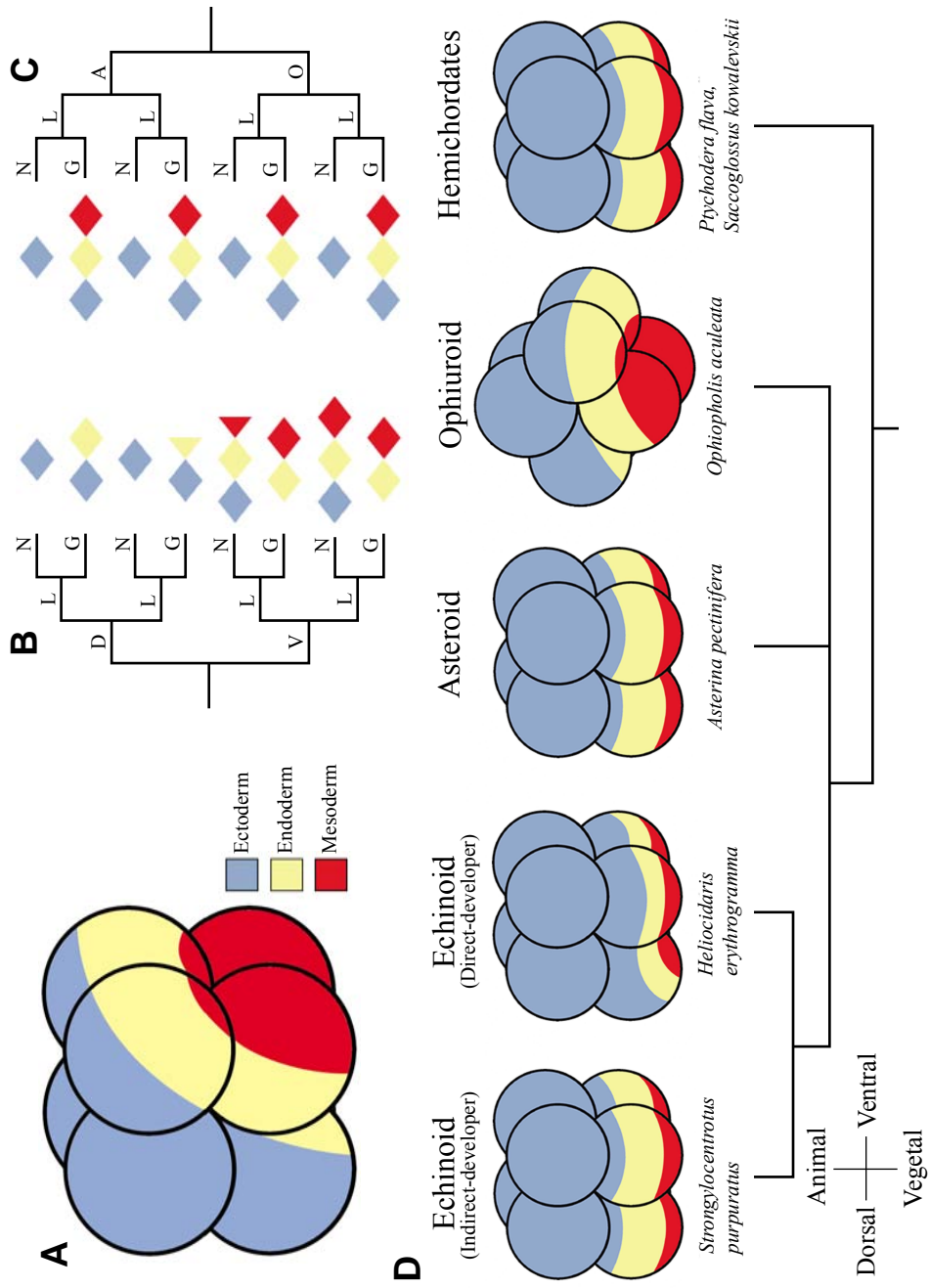Dorsal ——— Ventral

Animal

Vegetal

43

Table 2.3
Results of partial-embryo separations where both isolates survived

Stage and location of separation	Fate of isolate 1	Fate of isolate 2				Total pairs	Isolate origins confirmed[c]
	Ecto, Endo & Meso	Ecto, Endo & Meso	Ecto, Endo & Meso (Endo- & Meso-deficient)[a]	Ecto & Meso	Ecto		
2-cell stage along 1st cleavage plane[b]	27 (7)	0	20 (7)	0	7 (5)	27	12
4-cell stage along 2nd cleavage plane	22 (9)	22 (9)	0	0	0	22	0
8-cell stage along 3rd cleavage plane[b]	36 (18)	0	26 (18)	1 (1)	9 (8)	36	8

Note: Ecto = ectoderm; Endo = endoderm; Meso = mesoderm.
[a] These isolates clearly produced less endodermal and mesodermal derivatives than the other isolate in their pair.
[b] Isolate 1 and isolate 2 are predicted to be derived from more animal and more vegetal embryonic regions, respectively. These predictions are based on fate mapping results and confirmed in a number of cases (see Isolate origins confirmed[c]).
[c] Number of cases where the embryonic origin of each isolate was determined with a Nile blue marking technique.
() indicate the number of cases where the presence and/or absence of spicules and gut tissue were confirmed with polarized light and alkaline phosphatase staining, respectively.

Next, embryonic fragments were separated along the second cleavage plane at the 4-cell stage. In 11 cases, both isolates were still alive at the time of analysis. In each of these cases, both isolates gave rise to ectodermal, endodermal, and mesodermal derivatives, but in each case one isolate produced slightly more endodermal and mesodermal derivatives than the other (Fig. 2.8C,C').

Finally, embryonic fragments were separated along the third cleavage plane at the 8-cell stage. In 36 cases, both isolates were still alive at the time of analysis (Table 2.3). In 26 of these cases, both blastomeres gastrulated and gave rise to ectodermal, endodermal, and mesodermal derivatives, although one of the two isolates formed a significantly smaller gut than the other and a reduced larval skeleton (Fig. 2.8D,D'). In these endomesodermally-deficient isolates, formation of endoderm and mesoderm was also delayed with respect to controls. In 9 of these cases, one blastomere gastrulated and gave rise to a small but phenotypically normal larva while the other did not gastrulate and

gave rise to a hollow-ciliated ectodermal vesicle (Fig. 2.8E,E'). In 1 pair one isolate

gastrulated and gave rise to a small but phenotypically normal larva while the other did

not gastrulate and gave rise to only ectoderm and skeletogenic mesenchyme. In 8 of the

cases in which both isolates survived until the time of analysis one of the isolates was

marked with Nile blue at the 8-cell stage so that the embryonic origin of isolates could be

determined at the time of analysis. In each of these cases, the more vegetally-derived

isolate gave rise to more endodermal and mesodermal derivatives, regardless of whether

the animal (n=4) or vegetal (n=4) half of the embryo was originally labeled.

Discussion

Our knowledge of the developmental mechanisms that function in echinoderm

embryos is largely based on work conducted on sea urchins. Although some

experimental work has also been conducted on asteroids, virtually nothing is known

about the mechanistic basis of embryogenesis in other echinoderm classes. This is the

first experimental study conducted on any member of the echinoderm class Ophiuroidea.

Cell lineage of larval fates in O. aculeata

A fate map of the early *O. aculeata* embryo was produced through the 8-cell stage

(summarized in Fig. 2.7A,B). This fate map reveals how the early embryo is organized

and becomes partitioned: (1) all of the mesoderm and most of the endoderm segregate

from most of the ectoderm at first cleavage; (2) the orientation of the first cleavage plane

is invariant and frontal (i.e. it is perpendicular to the presumptive larval D-V axis); (3)

45

Fig. 2.8. Partial-embryo isolates stained for alkaline phosphatase (black) after 6-7 days of development. Letter pairs (for example A and A') represent isolate pairs derived from a single bisected embryo. (A,A',B,B') Isolates produced by separation of sister blastomeres at the 2-cell stage. (A) Small, normal larva. (A') Small, abnormal larva with disproportionately-small gut (note decreased alkaline phosphatase staining compared to A), and reduced larval skeleton (note only one arm). (B) Small, normal larva. (B') Hollow, ciliated ectodermal vesicle lacking endodermally-derived gut tissue (note lack of alkaline phosphatase staining) and mesodermally-derived skeletogenic mesenchyme (note lack of spicules). (C,C') Isolates produced by separation of embryonic-halves at the 4-cell stage along the second cleavage plane. Both isolates have produced a small larva with slightly reduced larval skeleton. One larva (C) appears to have produced slightly more skeletogenic- and gut-tissue than the other (C'). (D,D',E,E') Isolates produced by separation of embryonic-halves at the 8-cell stage along the third cleavage plane. (D) Small, normal larva. (D') Small, abnormal larva with disproportionately-small gut and reduced larval skeleton. (E) Small, normal larva. (E') Hollow, ciliated ectodermal vesicle lacking endodermally-derived gut tissue and mesodermally-derived skeletogenic mesenchyme. Scale bar 100µm.
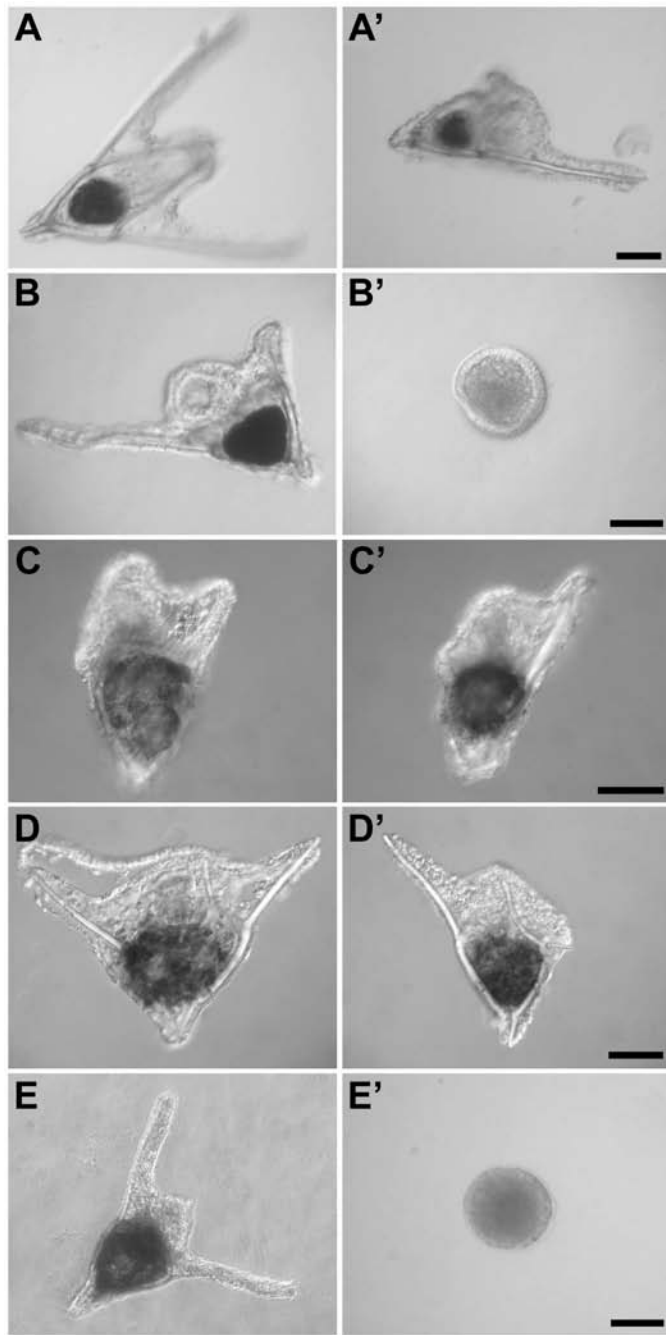
neither the first nor the second cleavage plane which forms in the dorsal blastomere

intersects the A-V axis of the embryo; (4) the second cleavage plane which forms in the

dorsal blastomere is oblique to the larval plane of bilateral symmetry. It should also be

noted that the exact location of the boundary of injected clones for a specific cell lineage

and the fates of some cells at the 4- and 8-cell stage vary slightly from embryo to embryo.

Despite this variability, a pattern of cell fates clearly emerged from these studies.

Although most fate mapping studies have not emphasized variability in their results, an

investigation specifically addressing this issue in an echinoid found significant variation

in the fates of specific cell lineages between embryos (Logan and McClay, 1997). Such

variability could be caused by variation in a number of different cytological factors, such

as the placement or angle of cleavage planes or the distribution of localized maternal

determinants; both have been observed here.

Cell lineage in echinoderm and hemichordate embryos

　　　　Before this study, fate maps had been produced for a number of non-chordate

deuterostomes including multiple echinoids (Cameron and Davidson, 1991; Cameron *et

al.*, 1987; Hörstadius, 1973; Wray and Raff, 1990), an asteroid (Kominami, 1983), and

two enteropneust hemichordates (Colwin and Colwin, 1951; Henry *et al.*, 2001).

Comparison of these fate maps indicates that they are all strikingly similar (Fig. 2.8C,D).

The only major deviation from the typical echinoderm-hemichordate cell lineage that had

previously been observed is in the direct-developing echinoid *H. erythrogramma* where

the presumptive endodermal and mesodermal contributions to the dorsal vegetal

48

blastomeres at the 8-cell stage appear to have decreased slightly with respect to other echinoderms and hemichordates (Wray and Raff, 1989, 1990). Minor differences within this clade may also include slight shifts of presumptive larval fates up and down the A-V axis (Henry *et al.*, 2001; Logan and McClay, 1997). Nevertheless, the similarity observed in echinoderm and hemichordate embryos previously examined has led some to believe that several cell lineage-specific features have been highly conserved within this group, perhaps as a consequence of developmental constraints (Raff, 1999). The data presented in this study indicate that the fate map of *O. aculeata*, and therefore the distribution of presumptive larval cell fates in these embryos, differs significantly from the fate map of other species within the echinoderm-hemichordate clade (Fig. 2.7B-D).

This study suggests that the novel cell lineage observed in *O. aculeata* is the consequence of an evolutionary shift in the orientation of first cleavage with respect to the A-V axis in these embryos. Although it is possible that measurements of cleavage plane angles with respect to the A-V may have been distorted by polar body slippage along the embryonic surface prior to analysis, Nile blue marking experiments support the findings that the first two cleavage planes do not interest the A-V axis. In these experiments, either the animal (A) or vegetal (V) pole was marked with Nile blue just after polar body expulsion; confidence in marking the A or V poles in these cases was very high. Marked A poles consistently give rise to the front tip of swimming blastulae and gastrulae, and marked V poles consistently give rise to the trailing end (vegetal plate) of blastulae and gastrulae; marks in both cases are centered well along the line of bilateral symmetry and anterior-posterior (A-P) axis (Fig. 2.3). While clonal boundaries of cells

injected at the 2-cell stage are typically bilaterally symmetrical, they never bisect Nile

bile marked regions and are clearly oblique to the A-P axis indicating that the first

cleavage plane is oblique to the A-V axis (Fig. 2.3C,D). Clonal boundaries of injected

dorsal-blastomere daughters at the 4-cell stage don't bisect Nile blue marked regions and

are clearly oblique to the line of bilateral symmetry indicating that the second cleavage

plane (in the dorsal blastomere at least) is also oblique to the A-V axis.

That cleavage planes may be uncoupled from embryonic axes without dramatic

consequence in terms of the progress of normal development is also supported in the

literature. In echinoderm embryos, experimentally altering the orientation of early

cleavage planes or the site of polar body expulsion does not alter embryonic axes; the site

of gastrulation always corresponds to the vegetal pole of the oocyte (Morgan and

Spooner, 1909; Shirai and Kanatani, 1980). Similar perturbations in *Xenopus* embryos

produce similar results, and naturally occurring variation in these embryos between the

orientation of first cleavage and embryonic axes demonstrate the pliability of early

cleavage planes and the importance of the A-V axis as a determining factor in the

establishment of embryonic polarity (Black and Vincent, 1988; Danilchik and Black,

1988).

Specification of larval fates in O. aculeata

A series of partial-embryo isolation experiments were performed in 2-, 4-, and 8-

cell embryos. These experiments indicate that the developmental potential to form

endoderm and mesoderm segregates unequally at the first three cleavages; this is

especially true for the first and third cleavages. Segregation of endodermal and mesodermal developmental potential, however, is not typically complete (i.e. both isolates form endoderm and mesoderm in over 74% and 72% of the cases for the first and third cleavages, respectively). The isolate associated with higher levels of endodermal and mesodermal potential is always the isolate derived from a more vegetal position.

In these experiments, many partial-embryo isolates followed their fate (i.e. they gave rise to what they would have given rise to in an unperturbed embryo, based on fate-mapping studies presented here). However, many partial-embryo isolates did not follow their fate. For example, the more animal blastomere in the 2-cell embryo—the dorsal blastomere—is fated to become ectoderm and endoderm. Dorsal blastomeres isolated at this stage gave rise to either ectoderm, endoderm and mesoderm or just ectoderm; in no cases did this isolate match its fate. The extent to which endodermal and mesodermal cell types formed from dorsal blastomere isolates might be explained as follows.

Fate mapping studies indicate that the dorsal blastomere should always receive some variable but limited amount of presumptive endoderm but never any presumptive mesoderm. For cases in which the dorsal blastomere gave rise to ectoderm, endoderm, and mesoderm, it is proposed that some of the presumptive endoderm became mesoderm, and some of the presumptive ectoderm became endoderm and/or mesoderm. Such trans-fating events may occur in the absence of an inhibitory signal that is typically received by this embryonic region in the development of an unperturbed embryo. For cases where the dorsal blastomere gave rise to just ectoderm, it is proposed that either a sub-threshold amount of endoderm was inherited by the dorsal blastomere or some inductive signal that

51

is typically received by this embryonic region during the development of an unperturbed embryo was not present in these cases. These interpretations appear reasonable since work has shown that multiple intercellular signals (both inductive and inhibitory) emanating from the vegetal pole of the embryo play fundamental roles in the regional specification of echinoid embryos (Hörstadius, 1973; Ransick and Davidson, 1993, 1995; Sweet *et al.*, 1999). Because the notch-delta signaling pathway mediates two of these three early inductive signaling events in echinoids (Sherwood and McClay, 1997, 1999, 2001; Sweet *et al.*, 1999, 2002), it will be interesting to see if it plays a similar role in ophiuroids.

Developmental potential in echinoderm and hemichordate embryos

Isolation experiments similar to those conducted in this study have been conducted in two enteropneust hemichordates (Colwin and Colwin, 1951; Henry *et al.*, 2001), one asteroid (Dan-Sohkawa and Satoh, 1978) and two other echinoids (Hörstadius, 1973) (Fig. 2.9). Blastomeres isolated at the 2- or 4-cell stage embryos from each of these except *H. erythrogramma* exhibit regulative development, forming small but phenotypically normal larvae. In contrast, only one of the blastomeres isolated at the 2-cell stage in embryos of the ophiuroid *O. aculeata* and the direct-developing echinoid *H. erythrogramma* is able to make a small but phenotypically normal larva, while the other blastomere gives rise to an endomesodermally-compromised vesicle/larva (data presented here, Henry and Raff, 1990). These results indicate that the potential to make endoderm and mesoderm segregate unequally at first cleavage in *O. aculeata* and *H.*
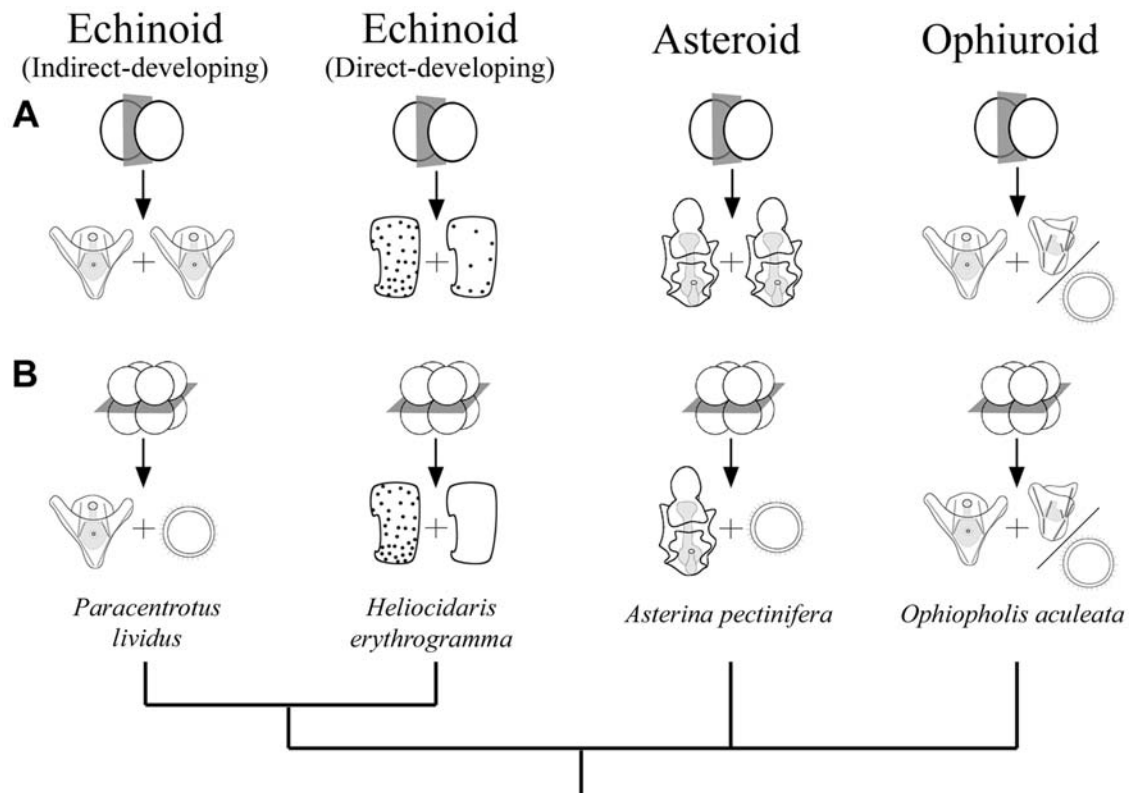
Fig. 2.9. Phylogenetic distribution of partial-embryo isolation experiments in early echinoderm embryos. Dots in *H. erythrogramma* represent pigment cells (mesodermally derived); endodermal derivatives not indicated for *H. erythrogramma*. (A) Blastomere isolations at the 2-cell stage. In the case of *O. aculeata*, the isolate on the left was ventrally-derived and the isolate on the right was dorsally-derived. (B) Partial-embryo isolation at the 8-cell stage along the third cleavage plane. In each case, the isolate on the left was vegetally-derived and the isolate on the right was animally-derived. Results for the two echinoids and asteroid are based on Hörstadius, (1973), Henry and Raff, (1990), Dan-Sohkawa and Satoh, (1978), Maruyama and Shinoda, (1990).

erythrogramma. Similar conclusions can be drawn for isolations of partial embryos separated along the second cleavage plane in *O. aculeata*. The inability of these two groups to fully regulate at these stages is likely a consequence of differences in larval fate contributions of early cell lineages rather than an indication that cell signaling plays a smaller role in these embryos. Whether these groups have employed novel regional specification mechanisms requires further investigation. At the 8-cell stage, vegetal halves isolated along the third cleavage plane develop into a small but normal larva and the corresponding animal halves develop into ciliated ectodermal vesicle in the asteroid and in both echinoid species (Henry and Raff, 1990; Hörstadius, 1973; Maruyama and Shinoda, 1990), indicating that in these embryos endomesodermal potential is retained in only the vegetal blastomeres at this stage. These experiments have not been conducted in hemichordates; however, isolates made along the third cleavage plane in *O. aculeata* typically produce endodermal and mesodermal derivatives, indicating that both halves retain the potential to make mesendoderm.

Embryological similarities between O. aculeata and H. erythrogramma

As discussed above, the embryos of the indirect-developing ophiuroid *O. aculeata* and the direct developing echinoid *H. erythrogramma* share a number of features that are otherwise unique to the echinoderm-hemichordate clade. These features include an unequal segregation of endodermal and mesodermal fates into the ventral blastomere at first cleavage (although this segregation is much more pronounced in *O. aculeata*), an unequal segregation of endodermal and mesodermal developmental potential into the

54

ventral blastomere at first cleavage, and a first cleavage plane that is invariantly frontal in orientation (Henry and Raff, 1990; Wray and Raff, 1989). This last trait is also shared with the echinoid *Holopneustes purpurescens* (Morris, 1995).

The presence of such similarities in these two disparate lineages within this clade is intriguing and leads one to ask a number of questions. First, why might these unique developmental features have been acquired in these two groups? One possibility is that these developmental features may have arisen because they are in some way selectively advantageous. For example, these changes may be associated with a mechanism which accelerates the process of D-V axis specification (Henry and Raff, 1990; Wray and Raff, 1990). Although there are arguments to the contrary (Hörstadius and Wolsky, 1936; Cameron *et al*., 1989), there is evidence that the D-V axis is not established until after the 4-cell stage in most echinoids (Pease, 1939; Hörstadius, 1973). The fact that both *O. aculeata* and *H. erythrogramma* embryos have an unequal segregation of endodermal and mesodermal developmental potential at first cleavage but no significant segregation in developmental potential at second cleavage indicates that determination of the D-V axis occurs by the 4-cell stage at the latest in both these groups. In fact, strong evidence indicates that the D-V axis is specified prior to first cleavage in *H. erythrogramma* (Henry *et al*, 1990). Alternatively, these changes may have allowed for the production of a more robust mechanism of D-V axis specification.

Second, how might these changes (particularly the changes in fate and developmental potential) have been mediated on a cellular level? This shift in the axis of developmental potential or fate with respect to A-V axis in *H. erythrogramma* may be the

result of either a movement of morphogenetic factors within the oocyte or an alteration in the pattern of cleavage divisions (Henry and Raff, 1990; Wray and Raff, 1990). In *O. aculeata*, it is shown here that the shift in developmental fates and potential in the embryo are the result of a shift in the cleavage program.

Conclusions

Recent comparative work on early embryogenesis in non-echinoid members of the echinoderm-hemichordate clade has produced a good deal of data suggesting that the mechanisms which underlie early development in this group are highly conserved. This work has focused on cell lineage (Wray and Raff, 1989, 1990), intracellular-signaling pathways (Kominami, 1984; Miyawaki *et al*., 2003), gene expression (Hinman and Davidson, 2003a, 2003b; Hinman *et al*., 2003b), and gene regulatory networks (Hinman *et al*., 2003a). The work reported here on the ophiuroid *O. aculeata* indicates that at least some processes of early development among echinoderms and hemichordates are subject to evolutionary change. Future experiments will be necessary to determine whether the differences in early development that exist between *O. aculeata* and other members of the echinoderm-hemichordate clade are just spatial rearrangements of identical developmental genetic architecture, or if the gene regulatory networks that underlie embryogenesis in *O. aculeata* and other members of the clade have in fact undergone evolutionary modification.

Appendix: Specification of germ layers and the dorsal-ventral axis in the early embryo of the brittle star *Ophiopholis aculeata*

Introduction

In most animal phyla at least one embryonic axis is defined prior to fertilization (Davidson, 1990; Melton, 1991). Such 'pre-specified' axes are based on organizational features imposed on an egg during oogenesis and are typically manifested by the polarization of localized maternal determinants in the egg. Embryonic axes that are not pre-specified are typically established via cell-cell interactions sometime after fertilization. In echinoid embryos the animal-vegetal (A-V) axis is established prior to fertilization. This has been demonstrated by cutting an echinoid oocyte into animal and vegetal halves. When fertilized the animal half produces an ectodermal ball with an animal tuft while the vegetal half produces an ovoid larva with ectodermal, endodermal, and mesodermal derivatives (Hörstadius, 1935). In echinoids the dorsal-ventral (D-V) axis (or oral-aboral axis) does not appear to be completed until sometime after the 8-cell stage in many echinoids, although this process may begin prior to 1st cleavage in these groups (Cameron *et al.*, 1989; Hörstadius, 1973). The mechanisms which underlie the establishment of the D-V axis and the specification of fates along the A-V axis are covered in more detail below.

Specification of fates along the A-V axis

Specification of cell fates along the A-V axis (and thus the specification of the three embryonic germ layers) in echinoid embryos is largely dependent on the signaling activity of the micromeres. Micromeres are produced at fourth cleavage by an unequal division of vegetal blastomeres. These cells give rise to skeletogenic cells or primary mesechyme cells (PMCs) and are specified autonomously (Cameron and Davidson, 1991; Okazaki, 1975). Micromeres recombined with animal halves of 8-cell stage embryos induced the animal halves to produce endoderm (Hörstadius, 1973). In the absence of micromeres animal halves produce ectodermal vesicles without endodermal or mesodermal structures. These experiments were interpreted to suggest that one of the roles of micromeres is to provide an inductive signal to the macromeres above them. These findings are supported by more recent experiments by Ransick and Davidson. If micromeres are transplanted to the animal pole of an embryo, these micromeres induce the formation of a second gut and ectopic expression of endodermal markers (Ransick and Davidson, 1993). Conversely, experiments where micromeres are removed shortly after they form demonstrate their importance for timely gut formation and the early expression of endodermal markers (Ransick and Davidson, 1995). In other recent experiments, removal of micromeres led to the absence of secondary mesenchyme cell (SMC) derivatives, and transplantation of micromeres to the animal pole results in the induction of ectopic SMCs (Sweet *et al*., 1999). Micromere-dependent signaling has been shown to be mediated by the notch-delta signaling system (Sherwood and McClay, 1997, 1999; Sweet *et al*., 2002). A third signal derived from the micromeres, also

mediated by notch and delta, also appears to play a role in positioning the endodermal-ectodermal boundary (Sherwood and McClay, 2001).

One of the first gene products to become asymmetrically distributed along the A-V axis of echinoid embryos is β-catenin. β-catenin becomes localized in the nuclei of the micromeres shortly after they are produced at 4th cleavage (Logan *et al*., 1999). After 5th cleavage, β-catenin localizes to the nuclei of macromeres as well. Over the next few cell divisions nuclear accumulation of β-catenin diminishes in the more-animal macromere lineages, but remains strong in the more-vegetal macromere progeny and micromere lineages. By a hatching-blastula stage, nuclear β-catenin is restricted to presumptive endodermal and mesodermal cells of the embryo (Logan *et al*., 1999). Nuclear accumulation of β-catenin in an asteroid is also restricted to vegetal blastomeres and follows a similar timeline (Miyawaki *et al*., 2003).

Several studies have demonstrated that β-catenin plays a central role in micromere signaling and the specification of cell fates along the A-V axis. Blocking nuclear localization of β-catenin throughout the embryo results in the formation of an 'animalized' phenotype, in which embryos fail to gastrulate or form any endodermal or mesodermal derivatives (Logan *et al*., 1999; Wikramanayake *et al*., 1998). Moreover, prevention of nuclear β-catenin accumulation in micromeres blocks both PMC differentiation (i.e. blastocoelar ingression and acquisition of skeletogenic capabilities) and the production of micromere derived signals (required for the production of endodermal-tissue and SMC formation) when grafted to an un-injected host (Logan *et al*., 1999; McClay *et al*., 2000). Over-expressing β-catenin on the other hand produces a

'vegetalized' phenotype, in which the number of endodermal and mesodermal cells and magnitude of endomesodermal gene expression are increased (Davidson *et al.*, 2002; Wikramanayake *et al.*, 1998). This vegetalized phenotype can be phenocopied by treating embryos with lithium chloride (LiCl) and is accompanied by an expanded domain of β-catenin nuclear localization (Hörstadius, 1973; Logan *et al.*, 1999; Nocente-McGrath *et al.*, 1991). In addition, animal-halves derived from embryos injected with a constitutively active form of β-catenin gastrulate and form endoderm whereas un-injected animal halves fail to gastrulate and form ectodermal spheres (Wikramanayake *et al.*, 1998).

The localization of β-catenin in vegetal nuclei is regulated by components of the canonical Wnt signaling pathway. During early cleavage, destabilization of a ubiquitously dispersed dishevelled (Dsh) protein in the animal pole of the embryo leads to the stabilization and nuclear localization of β-catenin in only the vegetal blastomeres of the embryo (Weitzel *et al.*, 2004). Dsh is thought to act by inhibiting glycogen synthase kinase-3β (GSK3β) which would otherwise phosphorylate β-catenin, targeting it for ubiquitination and protyolitic degradation (Cadigan and Nusse, 1997; Miller and Moon, 1996). Results from experiments in which wild-type and dominant negative forms of GSK3β were over-expressed in echinoid embryos are consistent with these findings (Emily-Fenouil *et al.*, 1998). In addition, it has been shown that the effect of LiCl on this pathway is a consequence of GSK3β inhibition (Hedgepeth *et al.*, 1997; Melton and Klein, 1996; Stambolic *et al.*, 1996). Although SpWnt8 signals reinforce and modify patterns of β-catenin nuclear localization during later cleavage stages, the initial pattern

60

appears to be regulated in a cell-autonomous manner (Davidson *et al*., 2002; Logan *et al*., 1999; Wikramanayake *et al*., 2004). In the nucleus, β-catenin functionally competes with the transcriptional-repressor LvGroucho for Tcf binding (Range *et al*., 2005). In association with orthodenticle (Otx), β-catenin-bound Tcf transcriptionally initiates a well-characterized vegetal signaling cascade which results in the specification of endomesodermal fates (Davidson *et al*., 2002; Huang *et al.*, 2000; Li *et al.*, 1999; Vonica *et al.*, 2000).

Because β-catenin and the canonical Wnt signaling pathway play a role in axial specification and/or germ layer segregation in ascidians (Imai *et al*., 2000), vertebrates (see Miller and Moon, 1996), *C. elegans* (Rocheleau *et al*., 1997; Thorpe *et al*., 1997), and possibly a cnidarian (Wikramanayake *et al*., 2003), and because of its' key role in endomesodermal specification in echinoids, the role that this pathway plays in *O. aculeata* was investigated. To examine the potential role of β-catenin in *O. aculeata* embryogenesis, the distribution of β-catenin was examined using an antibody against a sea urchin β-catenin. If β-catenin plays a role in endomesodermal specification in *O. aculeata*, one would expect it to accumulate selectively in the nuclei of presumptive endodermal and mesodermal cells. The effect of LiCl on endomesodermal specification was also examined. Lithium is a specific and potent inhibitor of β-catenin degradation so treatment with LiCl should up-regulate nuclear accumulation of this protein. If β-catenin positively regulates endomesodermal specification in *O. aculeata*, lithium-treatment should increase the amount of endomesodermal tissues produced.

Establishment of the dorsal-ventral axis

When the D-V axis is specified and/or established in echinoids has been a point of contention in the literature. Several lines of evidence suggest that D-V specification in echinoids begins very early in embryogenesis, perhaps even before fertilization. Lineage-tracer injection of single blastomeres at the two-cell stage of *Strongylocentrotus purpuratus* have shown that in this species the oral-aboral axis almost always lies 45 degrees clockwise to the first cleavage plane (Cameron *et al*., 1989). This strongly nonrandom association suggests that the oral-aboral axis has been specified prior to the first cell division. D-V asymmetries in respiratory activity and mitochondrial distribution can be seen in some echinoid oocytes and are good predictors of the D-V axis in both unperturbed and experimentally altered embryos (Coffman and Davidson, 2001; Coffman *et al*., 2004). On the other hand, the orientation of the first cleavage plane with respect to the plane of larval bilateral symmetry is much more variable in some echinoid (Henry *et al*., 1992; Hörstadius and Wolsky, 1936), asteroid (Kominami, 1983), and hemichordate (Henry *et al*., 2001) species, which may suggest that specification of the D-V axis in these may not begin until some later time. In addition, several lines of evidence indicate that establishment of the D-V axis is not completed until at least after the 8-cell stage. For example, individual blastomeres isolated from 4-cell embryos of multiple echinoid species give rise to small plutei with both oral and aboral parts (Driesch, 1892; Hörstadius, 1973).

Several approaches have been used to investigate the mechanistic basis of D-V specification in echinoids. One approach has used nickel chloride (NiCl$_2$), a potent inhibitor of D-V development in echinoids. *Lytechinus variegatus* embryos treated with nickel fail to acquire any asymmetries along the D-V axis (Hardin *et al*., 1992). Theses embryos appear morphologically normal through the early gastrula stage, but abnormalities begin to appear shortly thereafter. The ectoderm of normal embryos form two ventrolateral thickenings on which PMCs cluster to initiate the formation of the two larval spicule centers. In nickel-treated embryos, ventrolateral ectodermal thickenings become expanded to form a circumferential belt around the vegetal plate; PMCs form a ring along this ectodermal belt and initiate spiculogeneis in multiple centers in a radial pattern in the embryo. In normal embryos, the elongating archenteron typically bends to contact a thick portion of the ectoderm just ventral to the animal pole called the stomodeal invagination; these ultimately fuse to form the mouth of the larva. In nickel-treated embryos, the archenteron elongates directly towards the animal pole to contact a stomodeal invagination that has expanded to become a circumferential thickening around the animal pole. Immuno-fluorescence and *in situ* hybridization staining techniques indicate that the ciliated band is shifted to the vegetal margin of the embryo, the oral ectodermal domain is much larger and the aboral ectodermal domain is much smaller in nickel-treated embryos.

Another approach used to understand the mechanistic basis of D-V establishment has been a more direct analysis of candidate gene function. Analyses have identified a number of genes that are expressed in the ectoderm in a polarized manner along this axis

63

(Angerer *et al*., 2001; Croce *et al*., 2003; Gross and McClay, 2001). Functional tests have shown that several of these genes, including *nodal* and *BMP 2/4* (both members of the TGFβ superfamily), are required for establishment of the D-V axis (Angerer *et al*., 2000, 2001; Croce *et al*., 2003; Duboc *et al*., 2004; Flowers *et al*., 2004). Based on timing of expression and mis-expression analyses, *nodal* appears to be the most upstream of these. Nodal over-expression results in the production of a phenotype quite similar to nickel-treated embryos (radialization, over-expression of oral markers, etc.), yet *nodal* expression is radialized by nickel-treatment suggesting that it is the earliest known effecter of D-V establishment (Flowers *et al*., 2004; Duboc *et al*., 2004). Blocking BMP 2/4 expression with anti-sense morpholino oligonucleotides also phenocopies nickel-treatment suggesting that TGFβ signaling may be the target of nickel's radicalizing effect in sea urchins (Duboc *et al*., 2004).

Experiments in *O. aculeata* have shown: 1) that the first cleavage plane in this species is invariant and frontal (meaning that it is roughly perpendicular to a plane that divides dorsal from ventral), 2) that there is a major segregation of larval fates at first cleavage in this species such that one blastomere at the 2-cell stage gives rise to all the mesoderm, much of the endoderm, and a small potion of ventral ectoderm and the other blastomere gives rise to the remaining endoderm and ectoderm, and 3) that there is a major segregation of developmental potential at first cleavage in this species. These findings suggest that the D-V axis may be specified prior to first cleavage in *O. aculeata*. To test this hypothesis and to examine whether the mechanisms which underlie D-V specification in *O. aculeata* is similar to those employed by echinoids, *O. aculeata*

64

embryos were treated with $NiCl_2$ during early development. If D-V specification is mediated by similar proteins and/or signaling pathways, it is expected that treating *O. aculeata* embryos with LiCl will completely disrupt establishment of the D-V axis and radicalize embryos. If lithium does not have this effect, it suggests that the mechanistic basis for D-V establishment in *O. aculeata* has changed mechanistically and perhaps temporally.

Materials and Methods

Animals and embryos

O. aculeata adults were collected intertidally on San Juan Island, WA, and were maintained at 10-12 degrees C in aquaria with running sea water. To induce spawning, animals were exposed to a combination of bright light, heat and physical perturbation (shaking, swirling and/or inversion) for 1-2 hours. Animals were then placed in filtered sea water (FSW) at 12 degrees C in individual bowls; spawning took place within the next few hours. *Dendraster excentricus* and *Strongylocentrotus purpuratus* adults were collected by G. von Dassow and *Strongylocentrotus droebachiensis* adults were collected with the assistance of K. Zigler in the San Juan Islands, WA. Spawning was induced with an inter-coelomic injection of 0.55M KCl. Spawned oocytes were rinsed several times in FSW and fertilized with a dilute sperm concentration. Following fertilization embryos were rinsed several times and raised in either pasteurized Jamarin artificial sea water (JSW; Jamarin Labs, Osaka, Japan) or in filtered sea water (FSW). FSW was used to prepare lithium- or nickel-sea water solutions. In experiments with LiCl or $NiCl_2$ at

65

least 100 embryos were placed in each treatment group. In addition, each experiment

was conducted on embryos from at least two different spawned females; some

experiments were run 4-5 times.

Propidium iodide and phallacidin staining

Fluorescent dyes and confocal imaging were used to make cytological

observations. The fluorescent dyes used include propidium iodide (Sigma) and

BIODIPY FL phallacidin (Molecular Probes), which are nucleic acid-specific and

filamentous actin-specific, respectively. Embryos were fixed overnight in 4%

paraformaldehyde in JSW. Embryos were then rinsed in phosphate-buffered saline with

0.1% Triton X-100 (PBT), incubated in a PBT solution with 10 µg/ml propidium iodide

and/or 5 units/ml phallacidin, rinsed, dehydrated and cleared in benzyl benzoate and

benzyl alcohol (2:1). Stained samples were imaged with a BioRad Radiance 2000 laser-

scanning confocal microscope.

Immunocytochemistry

Embryos at stages prior to hatching were fertilized in JSW which contained para-

aminobenzoic acid and pulled into a small-bored pipette several times some time after

fertilization to remove their fertilization envelopes. These embryos were then fixed in

2.5% paraformaldehyde in JSW at room temperature (RT) for 20 minutes and

permiablized in ice cold 100% methanol for 10 minutes. Post-hatching stage embryos

were fixed in ice cold 100% methanol or 10 minutes. Embryos were then rinsed in PBT

with 1% bovine serum albumin and 5% normal goat serum and then 3 times in just PBT (rinses are for 5 minutes unless otherwise stated). Embryos were then incubated with a primary antibody for 1.5-2 hours at RT, rinsed 3 times in PBT, incubated in a secondary antibody for 1.5-2 hours at RT, rinsed 3 times in PBT and 1-3 times in PBS. Next embryos were deposited on poly-lysine coated slides, dehydrated in an ethanol series, cleared in a mixture of benzyl benzoate and benzyl alcohol (2:1) and mounted. Stained embryos were imaged with a confocal microscope as above. Primary antibodies included an affinity-purified anti-β-catenin polyclonal serum made against *Lytechinus variegatus* β-catenin as described previously (Miller and McClay, 1997) and an anti-β-catenin monoclonal antibody made against a chicken β-catenin (Sigma-Aldrich; C-7082). Secondary antibodies include an Alexa Fluor 568-conjugated goat anti-guinea pig IgG and an Alexa Fluor 488-conjugated donkey anti-mouse IgG (Molecular Probes; A11075 and A21202).

Quantitative analysis of cells

Embryos fixed and stained with propidium iodide and phallacidin were imaged with a laser-scanning confocal microscope as described above. In Image J, the two scanned channels were merged into a single stack of images and the Cell Counter plug-in was used to count ectodermal and endomesodermal cells. Cells were identified as 'ectodermal' if they were positioned in the external layer of the embryo. Cells were identified as 'endomesodermal' if they were positioned inside the blastocoel of these embryos. Microsoft Excel was used for statistical analysis.

Results

β-catenin Immunocytochemical Staining

Because β-catenin plays an important role in axial specification and germ layer segregation in a number of metazoan embryos including echinoids, the distribution of β-catenin protein was examined in *O. aculeata*. Prominent β-catenin staining was observed using the serum against *L. variegatus* β-catenin in gastrula stage embryos in adherens junctions, forming a ring in each epithelial cell at the boundary between the apical and lateral membrane domains (Fig. A.1 G-J). Throughout gastrulation, staining was present in epithelial but not mesenchymal cells even though many mesenchymal cells should be present at this stage. Many attempts were made to detect β-catenin protein in early cleavage and blastula stage embryos. These efforts included several protocol modifications. Attempts produced cleavage blastula and gastrula stage embryos that had a faint nuclear and/or cytoplasmic signal throughout the embryo, but in no case was this signal stronger than in negative controls (Fig. A.1 A-F). The antibody against a chicken β-catenin never produced a signal that was not seen in controls.

LiCl Treatment

To investigate the role of β-catenin and the canonical Wnt signaling pathway in regional specification during embryogenesis of *O. aculeata*, embryos were treated with various concentrations of LiCl in FSW during early development. Experiments in which embryos were treated with 50mM LiCl are discussed because higher concentrations

appeared to be toxic and lower concentrations produced very mild phenotypes. The vegetalizing effects of lithium on *L. variegatus* are observed when embryos are treated with 30-50mM LiCl from 0-10h (Logan *et al*., 1999).

In *O. aculeata*, lithium-treatment caused a number of developmental abnormalities. Embryos treated with lithium from 30 minutes after fertilization until 18 hours after fertilization (0-18h) developed much more slowly than controls did. These embryos did not become dorso-ventrally flattened at an early gastrula stage as did controls but remained radially symmetrical well into gatrulation. These embryos were also much shorter along the A-P axis during blastula and gastrula stages than controls and were broad and well-rounded at the animal pole through these stages (Fig. A.2 A,C). Embryos treated from 0-8h displayed a phenotype intermediate to controls and the longer treatment, both in timing and in shape. These embryos became pear-shaped during gastrula stages, having a narrower animal pole than the embryos treated for a longer period (Fig. A.2 A,B). Embryos in both of these treatment groups gastrulated and produced skeletogenic mesenchyme. Archenterons produced during gastrulation were directed into the blastocoel (no cases of exogastrulation were observed) and spicules that formed typically elongated and often produced a larval skeleton which resembled that of controls in 0-8h embryos (Fig. A.2 D,E). Embryos in the 0-18h treatment group also produced elongate spicules, although sometimes 4-6 spicule centers formed (Fig. A.2 D-F). These embryos also appeared to be compressed along the D-V axis. All treated embryos formed ciliated-bands which ran along their mid-ventral surface and then anteriorly. Although archenterons produced in embryos from the 0-8h treatment group

69

Fig. A.1. Expression of ß-catenin protein in *O. aculeata* embryos based on immunohistochemical localization with an anti-*L. variegatus* ß-catenin serum. (A,D,G,I) Single confocal sections. (B,C,E,F,H,J) Projections of confocal stacks. (A-C) 64-cell stage embryos. (D-F) 128-cell stage embryos. (G,H) Early-gastrula stage embryos. (I,J) Late-gastrula stage embryos. (C,F) Negative controls which were processed the same as stained embryos except they were not incubated with anti-*L. variegatus* ß-catenin serum. Scale bar indicates 25 µM.
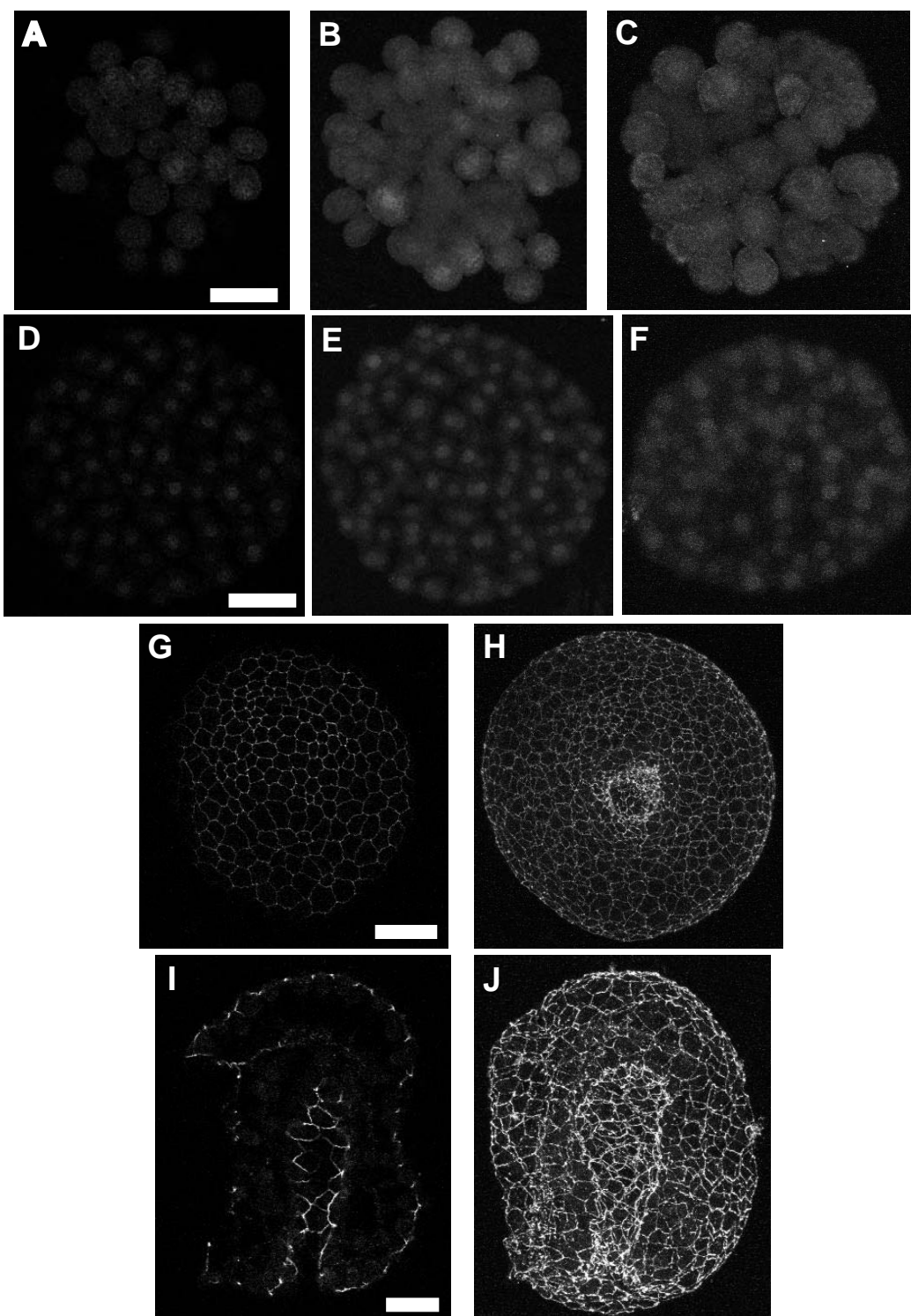
Fig. A.2. Lithium-treated *O. aculeata* embryos. (A) Untreated controls at 42 hours had formed a mid-gastrula stage, had started producing spicules and were compressed along their D-V axis. (B) Embryos treated from 0-8h had begun gastrulation and spiculogenesis but were pear-shaped at 42 hours. (C) Embryos treated from 0-18h had not formed an archenteron and had not begun spicule production but did appear to contain mesenchyme cells by 42 hours. These embryos were also much shorter along the A-P axis than controls and completely radially symmetrical. (D) Untreated controls at 5 days had formed 2-armed plutei with a well developed skeleton, a tripartite thru-gut and ciliated band. (E) Embryos treated from 0-8h formed plutei similar to controls by 5 days, although they looked younger than controls and often showed R-L asymmetries. (F) At 5 days, embryos treated from 0-18h resembled much earlier controls that had more depth along the D-V axis. These embryos often contained extra, stunted spicule centers.
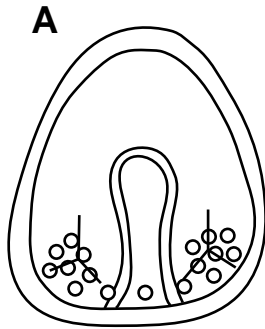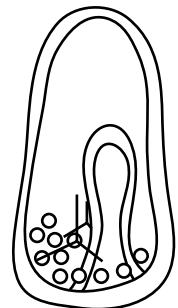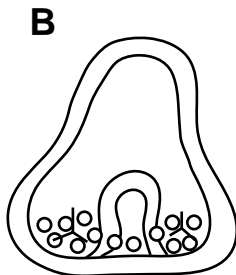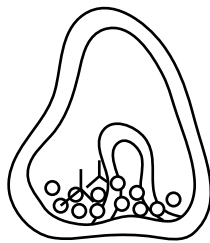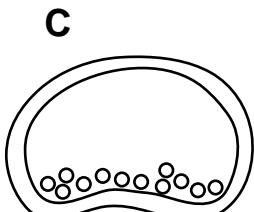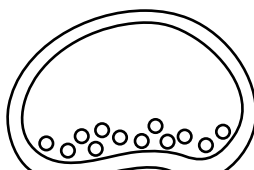
A

Ventral view   Lateral View

B

Ventral view   Lateral View
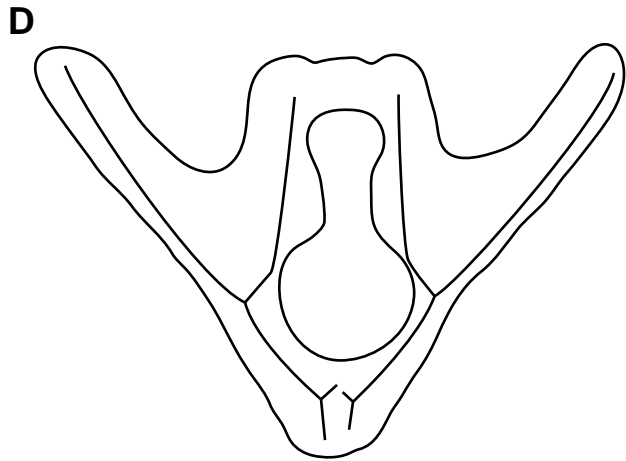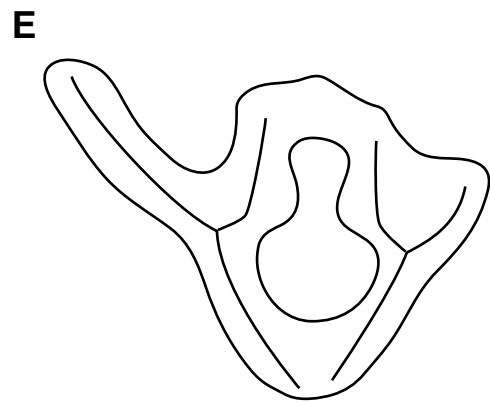
C

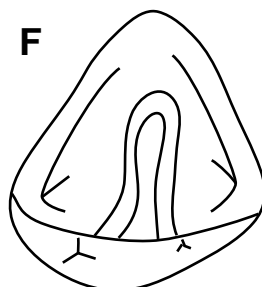Ventral view   Lateral View

D

Ventral view

E

Ventral view

F

Ventral view   Lateral View

gave rise to thru-guts, it is unclear whether the archenterons of embryos in the 0-18h treatment group fused with the ectoderm to form a mouth.

To see if there was an increase in the in the production of endomesoderm in lithium-treated embryos, the number of ectodermal and endomesodermal cells in embryos treated from 0-15h were counted. Embryos were examined at a late-gastrula stage just after the two feeding arms began to form in controls (40 hours post-fertilization). This stage was ideal for such an analysis because a good deal of endoderm and mesoderm had already formed, the number of cells present in the embryo was still reasonable and cells were easily identifiable as 'ectodermal' or 'endomesodermal' at this stage. The average number of cells/embryo and the percentage of cells in the presumptive endomesoderm differed between the control and treatment groups (Table A.1). Specifically, the number of cells in lithium-treated embryos was lower than in controls. These findings are consistent with a slightly delayed program of development in lithium-treated embryos, as was reported earlier. More importantly, however, the proportion of endomesodermal cells in lithium-treated embryos was higher than in controls. Although sample sizes were small, this difference was shown to be significant as measured by a one-tail t-test ($t = 2.584$; $p = 0.025$; df = 5).

NiCl$_2$-treatment

Morphological indications of a secondary embryonic axis become apparent in *O. aculeata* at between 30-35 hours post-fertilization, shortly after gastrulation begins. The first signs of a secondary axis are a flattening of the embryo along the D-V axis so that it

Table A.1
Effect of LiCl-treatment on developmental rate and endomesodermal specification in *O. aculeata*

	Number of cells in embryo		Percentage of cells in Endomesoderm	
	Average	Range	Average	Range
Controls (n = 3)	722	635-790	21.5%	18.9-23.9%
50mM LiCl (n = 4)	542	471-596	33.4%	22.7-40.2%

becomes wider from left-to-right than it is thick from dorsal-to-ventral by a ratio of

approximately 3:1. The first clear D-V asymmetries include a dorsally-positioned

archenteron and two ventral and lateral clusters of mesenchyme cells (see Fig. A.2 A).

These mesenchymal clusters are the sites were spicules initially form. Subsequently, the

elongating archenteron will bend ventrally and contact the stomodeum on the ventral

surface of the larva where the mouth will form (see Fig. 2.4). Elongating spicules also

create asymmetries along this axis as they start shaping the presumptive larva; most

significantly, growing spicule rods underlie the formation of the laterally and ventrally

projecting arms. Spicules also extend posteriorly and ultimately bring the anus to a more

ventral position than at earlier stages. At the same time, the ciliated ectodermal-band

begins to form which will roughly divide the dorsal and ventral surfaces along the

anterior edge of the larva and the anterior and posterior halves of the larva on the ventral

surface. Once formed, the ciliated-band represents a boundary between the oral ectoderm

(which surrounds the mouth and is located anteriorly on the ventral surface) and the

aboral ectoderm (which covers the posterior part of the ventral surface and the entire

dorsal surface of the larva) (see Fig. 2.4).

To determine whether $NiCl_2$ has any effect on the specification of the larval D-V axis

in *O. aculeata*, embryos were grown in filtered sea water containing dissolved $NiCl_2$ for

varying periods of time during early development. Embryos were treated from 30 minutes after fertilization until either 24 or 45 hours after fertilization (0-24h or 0-45h, respectively) or from 24-52h. The concentration of $NiCl_2$ in FSW was varied and ranged from 0.125-2.0mM. Development of embryos in all treatment groups appeared normal morphologically through a mid-gastrula stage, although some of the treatment groups showed slight developmental delays.

By 42 hours control embryos had become swimming mid- to late-gastrulae. These embryos were flattened along the D-V axis and showed clear signs of asymmetry along this axis in the form of mesenchymal clusters and newly forming spicules positioned ventrally along the vegetal plate and the elongating archenteron positioned dorsally. Development in all nickel-treated embryos is delayed, although the extent of the delay is dependent on the amount of nickel exposure. Embryos treated with concentrations of $NiCl_2$ at 0.5mM or higher for 0-43h or concentrations of $NiCl_2$ at 1.0mM or higher from 0-24h were just beginning to gastrulate and had produced no spicules; embryos in all other treatment groups had begun to gastrulate and produce spicules, but to lesser extents than controls. Embryos treated with 0.5mM $NiCl_2$ from 0-24h or with lower concentrations of $NiCl_2$ were flattened along the D-V axis and showed signs of asymmetry along this axis, although to a lesser extent than controls. Embryos treated with 0.5mM $NiCl_2$ from 0-45h or 24-52h or with higher concentrations of $NiCl_2$, on the other hand, were radially symmetrical around the A-V axis.

By 66 hours control embryos had formed tri-partite thru-guts and had begun to produce feeding-arms supported by elongating spicules. A well formed ciliated band had

76

not formed at this point. By 66 hours all nickel-treated embryos that were still alive were showing signs of asymmetry along the D-V axis. Almost all embryos treated with 0.125mM $NiCl_2$ from 0-24h resembled slightly earlier stages of control embryos; these embryos had formed thru-guts and produced spicules which had started to elongate. Many embryos belonging to the other treatment groups also resembled earlier stages of controls. These embryos had formed archenterons which continued to elongate and contained birefringent material. None of the archenterons in these embryos had fused to form thru-guts nor had any of the birefringent masses become elongated spicules. Some embryos in these other treatment groups, particularly in groups treated from 0-43h or with concentrations of $NiCl_2$ exceeding 0.25mM, did not resemble controls at any stage particularly well; the proportion of abnormal development per treatment group increased with increasing $NiCl_2$ concentration. Abnormal embryos typically contained mesenchyme cells and an archenteron enclosed within an ectodermal sheet but was more pear-shaped than controls. Most of the embryos treated with 2.0mM $NiCl_2$ were either dead or extremely abnormal and falling apart at this stage. It should be reiterated that all of the live and intact $NiCl_2$-treated embryos observed at 66h had an asymmetric distribution of mesenchyme and birefringent material to one side of the vegetal plate of the embryo (presumable ventral) and an archenteron emerging from the other side of the vegetal plate (presumably dorsal). In none of these cases were embryos radially symmetrical.

   At 4 days of development controls had reached an early larval stage with two feeding arms and a well-formed ciliated band. The phenotypes of viable nickel-treated embryos

at this stage were variable both within and between treatment groups (Fig. A.3). Treatments at 0.5mM concentrations and higher are discussed more thoroughly below. Although nickel–treatment did not typically prevent the production of spicules, this treatment did severely affect the types of spicules that were produced. Specifically, many spicules that did form did not elongate but rather become birefringent granules. It was not uncommon to find more than 4-6 birefringent granules per embryo; this was also the case for 66h embryos. Some spicules did elongate, but were severely truncated. Nickel-treatment also affected gut formation. While well-defined archenterons were almost always present, they were often shorter than they were in controls (approximately two-thirds to three-fourths the length of control archenterons at the time of fusion to the stomodeum), they did not bend ventrally, and they did not fuse with the stomodeum to form a mouth. Nickel-treatment also affected the positioning of the ciliated band and it did so in a concentration-dependent manner. These defects are all indicative of improperly patterned ectoderm. Based on the position of the ciliated band, it appears that there may have been an expansion of the oral ectoderm in nickel-treated embryos. Despite these defects, asymmetries along a secondary embryonic axis were apparent in larvae of all treatment groups at this stage. Even in the most abnormal larvae, mesenchyme and spicules were at one side of the vegetal plate while the archenteron emerged from the other.

It was previously shown that nickel-treatment completely disrupts D-V specification in the embryo of the echinoid *L. variegatus* at concentrations as low as 0.5mM even if only applied from a hatching blastula to a late-gastrula stage (Hardin *et al.*, 1992). To
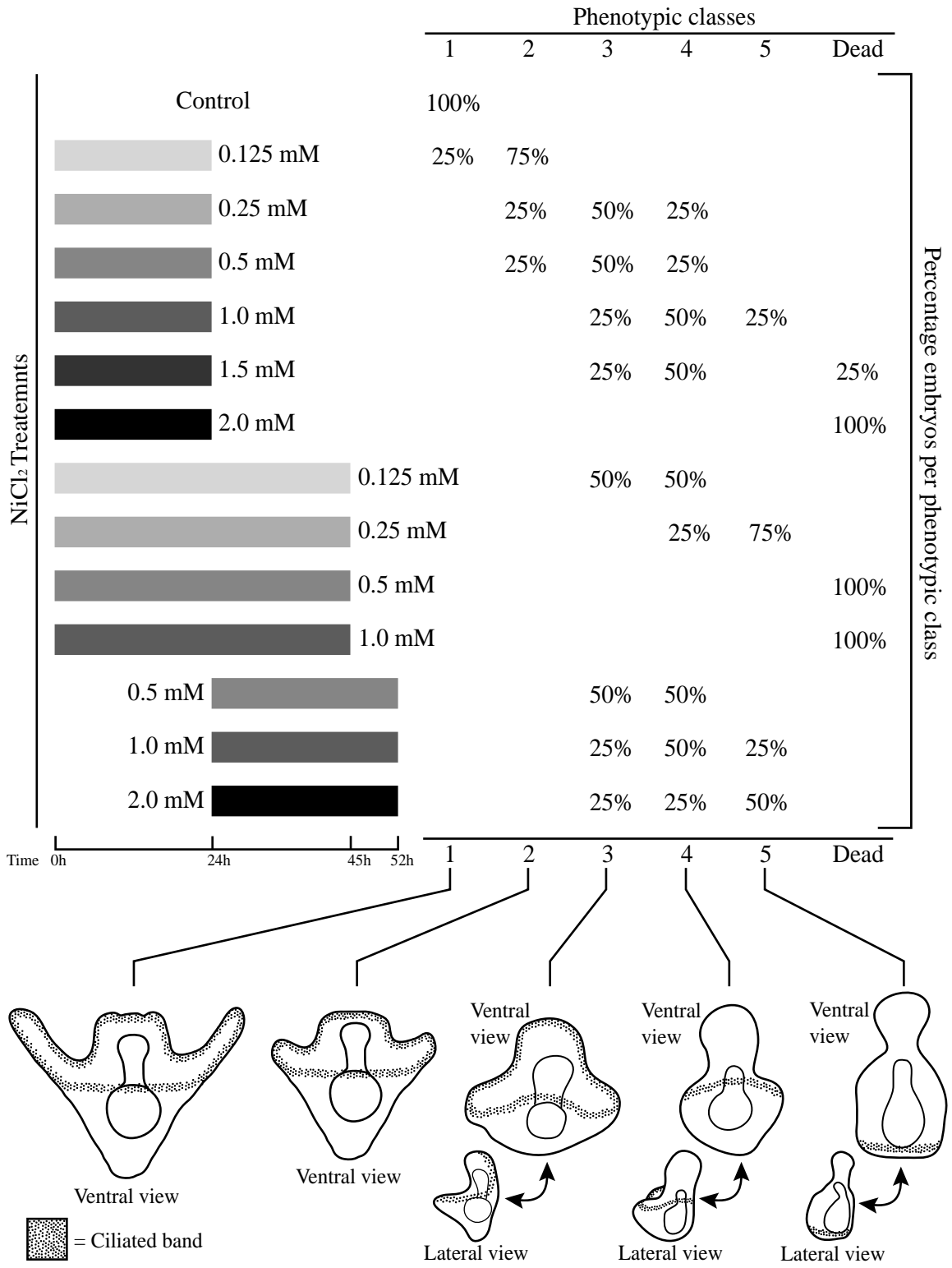
78

examine the effect of NiCl$_2$ on D-V specification in other echinoids and the sensitivity of these embryos to NiCl$_2$, the embryos of three previously unexamined echinoids (*D. excentricus*, *S. droebachiensis* and *S. purpuratus*) were treated with NiCl$_2$ in a manner similar to *O. aculeata* above. Although some minor phenotypic differences did exist between these echinoid species in response to nickel-treatment, embryos of each of these groups treated with 0.5mM NiCl$_2$ from 0-24h showed a completely radialized phenotype. These results suggest that the effect of nickel on echinoids is not specific to *L. variegatus* and that NiCl$_2$ is effective at concentrations as low as 0.5mM for 24 hour treatments.

Discussion

β-catenin and patterning along the animal-vegetal axis

β-catenin has two distinct functions in metazoan cells; it can contribute to cell-cell adhesion by acting as a cytoskeletal linker molecule in the cytoplasm or it can function as a regulator of gene activity via direct interactions with DNA-binding transcription factors in the nucleus (for review see Cadigan and Nusse, 1997; Miller and Moon, 1996). In fact, β-catenin clearly plays both roles in echinoid embryos. Shortly after 5th cleavage β-catenin localizes within the nuclei of vegetal blastomeres where it is thought to transcriptionaly activate an endomesodermal gene network (Davidson *et al*., 2002; Logan *et al*., 2001). β-catenin also associates with lateral cell-cell contacts and accumulates at adherens junctions from early cleavage stages through embryogenesis where it is thought to mediate cell adhesion (Miller and McClay, 1997). At gastrulation, changes in β-

Fig. A.3. Phenotypic effects of $NiCl_2$-treatmet on *O. aculeata* embryos at 4 days of development. Several different phenotypic classes have been defined (indicated with the numbers 1-5: 1 represents a normal phenotype and 5 represents the most abnormal phenotype). Although many larvae resemble intermediates between these defined groups, this classification scheme should allow a rough quantification of the phenotypes produced by different $NiCl_2$-treatments. The term 'larva' is used to describe all viable products of these treatments, although many of these products more closely resemble abnormal embryos. Class 1 includes larvae which are similar to control embryos. Class 2 includes larvae which closely resemble earlier stage control larvae with a well defined and properly positioned ciliated band, a tri-partite through-gut and arms supported by spicules; the arms of larvae in this class are less th an half the length of arms of controls. Classes 3-5 include larvae which form archenterons which elongate but do not fuse with the stomodeum to form a mouth. Larvae in classes 3-4 produce spicules that elongate to support short larval arms occasionally on one side of the larva but not the other; the other side often produces spicule granules which do not elongate. Larvae in these classes also have well-formed ciliated bands. The major difference between class 3 and class 4 larvae is the placement of the ciliated band. Larvae in class 3 have a normally positioned ciliated band; part lies long the anterior edge of the larva separating dorsal from ventral and the remainder runs from left to right on the ventral surface half way between anterior and posterior ends of the larva. The ciliated band in larvae of class 4 basically creates a ring around the larva half way between the anterior and posterior ends of the larva. Class 5 larvae typically have poorly-formed ciliated bands that are positioned very close to the blastopore (at essentially the posterior end of the larva). Larvae in this class often do produce spicule granules, but these granules never elongate. The number of spicules initiated in an embryo was highly variable and did not correspond well to the class in which that embryo was placed.

Phenotypic classes

NiCl$_2$ Treatments	1	2	3	4	5	Dead
Control	100%					
0.125 mM	25%	75%				
0.25 mM		25%	50%	25%		
0.5 mM		25%	50%	25%		
1.0 mM			25%	50%	25%	
1.5 mM			25%	50%		25%
2.0 mM						100%
0.125 mM			50%	50%		
0.25 mM				25%	75%	
0.5 mM						100%
1.0 mM						100%
0.5 mM			50%	50%		
1.0 mM			25%	50%	25%	
2.0 mM			25%	25%	50%	

Percentage embryos per phenotypic class

Time 0h   24h   45h 52h

1   2   3   4   5   Dead

Ventral view

Ventral view

Ventral view

Lateral view

Ventral view

Lateral view

Ventral view

Lateral view

= Ciliated band

catenin localization accompany several morphogenetic events. These include a complete loss of peripheral β-catenin in cells undergoing an epithelial-to-mesenchymal transition (in the formation of PMCs and SMCs) and a significant decrease in adherens junction-associated β-catenin levels in epithelial cells of the archenteron as they undergo convergent-extension movements (Miller and McClay, 1997).

Although nuclear localization of β-catenin was not detected in *O. acuelata*, β-catenin protein was found to be localized along the cell-cell boundaries of epithelial cells in gastrula stage *O. aculeata* embryos. β-catenin is probably functioning in these cells as a mediator of cell adhesion. This hypothesis is supported by the fact that detectable levels of β-catenin were present in all epithelial cells but no mesenchymal cells of the embryo at this stage. Since it is unclear from this analysis whether β-catenin was present in presumptive mesenchyme cells prior to their ingression, it can not be determined whether changes in β-catenin localization may have mediated this morphogenetic transition. Changes in the intensity of β-catenin associated with convergent-extension movements of the archenteron were not observed in *O. aculeata*, which may indicate that significant changes in the process of archenteron elongation have taken place between echinoids and ophiuroids.

The absence of β-catenin accumulation in adherens junctions prior to gastrulation suggests that β-catenin does not mediate cell adhesion by functioning in adherens junctions during cleavage and blastula stages. This idea is supported by the fact that cells in embryos of this species (and many other ophiuroid species) do not appear to adhere to each other tightly until some time near the beginning of gastrulation. In several

ophiuroids including *O. aculeata*, blastomeres are often very loosely associated and it is thought that these cells are essentially kept from falling apart by a very thick hyaline layer (Olsen, 1942). Although it is not known when cadherin-catenin complexes begin to function in these embryos, these data suggest this may not occur until around gastrulation. The absence of β-catenin accumulation in nuclei at any embryonic stage suggests that β-catenin does not mediate early specification events by acting as a nuclear transcriptional regulator in *O. aculeata*.

Lithium-treatment in O. aculeata

Lithium-treatment produced a number of developmental abnormalities in *O. aculeata* embryos; development was delayed, gastrula stages were stouter along the A-V axis and less flat along the D-V axis than controls, spicules were sometimes truncated and a mouth did not always form. Many aspects of development, however, proceeded in a normal (although delayed) manner; skeletogenic mesenchyme was produced, gastrulation took place, skeletal elements were properly patterned, and a ciliated band formed. These finding are not indicative of any major patterning defects in *O. aculeata* in response to LiCl. Moreover, the abnormalities observed in *O. aculeata* were largely inconsistent with the abnormalities seen in lithium-treated echinoid embryos. Echinoid embryos treated with even lower concentrations of LiCl for similar amounts of time typically exogastrulate (presumably due to a production of excess endoderm), form severely truncated spicules (if any spicules form at all), do not form a ciliated band and

83

lack indications of ectodermal patterning along a D-V axis (Hörstadius,1973; Nocente-McGrath *et al*., 1991, Wikramanayake *et al*., 1998).

The only clear similarity between the lithium-treatment phenotypes of echinoids and *O. aculeata* is that both appear to produce an excess of endodermal and/or mesodermal cells, although the magnitude of this change is larger in echinoids. In an asteroid, lithium-treatment also produces gastrulae with larger archenterons and fewer ectodermal cells than controls (Kominami, 1984). However, these results are similar to the results in *O. aculeata* in that they could be explained by other mechanisms. For example, it is possible that the increased proportion of endomesodermal cells in *O. aculeata* following LiCl-treatment was a function of lithium slowing down development if cell division in the ectoderm increases with developmental time.

The results of these experiments and the lack of nuclear β-catenin accumulation in *O. aculeata* embryos suggest that β-catenin does not play a role in endomesodermal specification in this group. To more conclusively address the role of β-catenin in *O. aculeata* embryogenesis one would need to clone β-catenin from *O. aculeata*, establish the spatial and temporal expression of the β-catenin transcript throughout embryogenesis, over-express an activated form of β-catenin and block its' nuclear accumulation (which would require cloning a cadherin gene). Given the amount of time and effort that would be involved in this process, the data here indicate that a more thorough analysis of this situation may not be worthwhile.

Dorsal-ventral axis specification and nickel-treatment in O. aculeata

Nickel-chloride is a potent inhibitor of D-V establishment in echinoid embryos. Most of the observed abnormalities in nickel-treated echinoid embryos take place in, or are potentially a consequence of defects in ectodermal patterning: typically polarized ectodermal thickenings expand radially to become rings, the ciliated band becomes restricted to a circumferential vegetal region, the oral ectodermal domain expands, the aboral ectodermal domain contracts, PMCs become distributed radially and the archenteron extends directly toward the animal pole.

Nickel-chloride also has a number of effects on embryogenesis in *O. aculeata*. Many of these defects may reflect abnormalities in ectodermal patterning. Nickel-treatment effects the placement of the ciliated band in a concentration dependent manner. At higher concentrations the ciliated band is restricted to a more vegetal, radialized position in the embryo, similar to the situation in nickel-treated echinoids. The archenterons of nickel-treated embryos are slightly truncated, do not bend ventrally, and do not fuse with the stomodeum. Because the final phase of archenteron elongation and thus archenteron-stomodeal fusion in echinoids appears to be dependent upon interactions between SMCs on the tip of the archenteron and a target ectodermal region near the animal pole (Hardin, 1988; Hardin and McClay, 1990), these findings could be explained by defects in either the SMCs or in the target ectoderm. No clearly identifiable stomodeum was observed in nickel-treated embryos in these treatment groups. However, because *O. aculeata* embryos are quite opaque, the stomodeum is not always readily apparent in normally developing embryos. Nickel-treatment also affected the proper

85

production of a larval skeleton in *O. aculeata*. Because there was no readily apparent decrease in the number of mesenchyme cells and birefringent material was almost always produced, the absence of normal skeleton formation was probably not because PMCs were not present. Because interactions between PMCs and the ectoderm have been shown to play a crucial role in skeleton formation in echinoids (Wolpert and Gustafson, 1961; Zito *et al*., 1998), a more viable explanation may be that certain ectodermal patterning cues that are necessary for skeletal development were either improperly expressed or not expressed at all.

Despite the nickel-induced abnormalities present in *O. aculeata* embryos described above, nickel-treatment never completely radialized *O. aculeata* embryos. Even the most extreme treatments of $NiCl_2$ that produced viable larvae did not prevent the formation of some signs of a secondary axis in *O. aculeata*. The blastopore was always asymmetrically positioned on one side of the vegetal plate while mesenchyme cells and spicules were asymmetrically positioned on the other. Several reasonable possibilities could account for this. One possibility is that D-V development occurs at the same time and has the same mechanistic basis in echinoids and *O. aculeata* but that $NiCl_2$ does not have the same proximal molecular/biochemical effect in *O. aculeata* as it does on echinoids. For example, perhaps $NiCl_2$ specifically inhibits some gene product in echinoids that is involved in D-V development in both groups but the same gene product in *O. aculeata* is somehow resistant to inhibition by $NiCl_2$. Several lines of evidence, however, argue against this. First, $NiCl_2$–treatment radialized all four different echinoid species examined. If genetic differences are to be the explanation of different phenotypic

differences between echinoids and *O. aculeata*, one might expect to see larger phenotypic differences between these genotypically divergent echinoid species. Second, such a possibility does not account for some of the similar phenotypic effects that $NiCl_2$ does have on these two different groups. Alternatively, it is possible that some aspects of D-V development share a mechanistic basis between these two groups but that others do not. If those mechanisms that are sensitive to $NiCl_2$ play a more significant role in echinoids, this might explain why a more severe phenotype is seen in this group. This possibility would more reasonably account for similar phenotypic effects between the groups and would also explain the differences. This possibility would also be consistent with a shift of at least some parts of the process of D-V specification to an earlier stage of development.

To address the mechanisms which underlie D-V establishment in *O. aculeata* more conclusively, there are several genes that could be cloned (BMP 2/4, nodal, brachyury, etc.). Once cloned spatial and temporal patterns of expression would need to be established and both over-expression and mis-expression assays would need to be performed. In addition, to more aptly be able to describe abnormal phenotypes, molecular markers which can be used to identify different tissue types (such as oral ectoderm, aboral ectoderm, skeletogenic mesenchyme, endoderm, etc.) need to be produced and/or characterized.

Bibliography

Angerer, L.M., Angerer, R.C., 2003. Patterning the sea urchin embryo: gene regulatory networks, signaling pathways, and cellular interactions. Curr. Top. Dev. Biol. 53, 159-198.

Angerer, L.M., Oleksyn, D.W., Levine, A.M., Li, X., Klein, W.H., Angerer, R.C., 2001. Sea urchin goosecoid function links fate specification along the animal-vegetal and oral-aboral embryonic axes. Development 128, 4393-404.

Angerer, L.M., Oleksyn, D.W., Logan, C.Y., McClay, D.R., Dale, L., Angerer, R.C., 2000. A BMP pathway regulates cell fate allocation along the sea urchin animal-vegetal embryonic axis. Development 127, 1105-14.

Angerer, L.M., Newman, L.A., Angerer, R.C., 2005. SoxB1 downregulation in vegetal lineages of sea urchin embryos is achieved by both transcriptional repression and selective protein turnover. Development 132, 999-1008.

Black, S.D., Vincent, J.P., 1988. The first cleavage plane and the embryonic axis are determined by separate mechanisms in Xenopus laevis. II. Experimental dissociation by lateral compression of the egg. Dev. Biol. 128, 65-71.

Boveri, T., 1901. Die polarität von ovocyte, ei, und larve des *Strongylocentrotus lividus*. Zool. Jahrb. Abt. Anat. U. Ont. 14, 630-653.

Cadigan, K.M., Nusse, R., 1997. Wnt signaling: a common theme in animal development. Genes Dev. 11, 3286-305.

Cameron, C.B., Garey, J.R., Swalla, B.J., 2000. Evolution of the chordate body plan: new insights from phylogenetic analyses of deuterostome phyla. Proc. Natl. Acad. Sci. USA 97, 4469-4474.

Cameron, R.A., Davidson, E.H., 1991. Cell type specification during sea urchin development. Trends Genet. 7, 212-218.

Cameron, R.A., Fraser, S.E., Britten, R.J., Davidson, E.H., 1989. The oral-aboral axis of a sea urchin embryo is specified by first cleavage. Development 106, 641-647.

Cameron, R.A., Hough-Evans, B.R., Britten, R.J., Davidson, E.H., 1987. Lineage and fate of each blastomere of the eight-cell sea urchin embryo. Genes Dev. 1, 75-85.

Coffman, J.A., Davidson, E.H., 2001. Oral-aboral axis specification in the sea urchin embryo. I. Axis entrainment by respiratory asymmetry. Dev. Biol. 230, 18-28.

Coffman, J.A., McCarthy, J.J., Dickey-Sims, C., Robertson, A.J. 2004. Oral-aboral axis specification in the sea urchin embryo II. Mitochondrial distribution and redox state contribute to establishing polarity in Strongylocentrotus purpuratus. Dev. Biol. 273, 160-71.

Colwin, A.L., Colwin, L.H., 1950. The developmental capacities of separated blastomeres of an enteropneust, *Saccoglossus kowalevskii*. J. Exp. Zool. 115, 263-296.

Colwin, A.L., Colwin, L.H., 1951. Relationships between the egg and the larva of *Saccoglosus kowalevskii* (Enteropneusta): axes and planes; general perspective significance of the early blastomeres. J. Exp. Zool. 117, 111-138.

Croce, C., Lhomond, G., Gache, C., 2003. Coquillette, a sea urchin T-box gene of the Tbx2 subfamily, is expressed asymmetrically along the oral-aboral axis of the embryo and is involved in skeletogenesis. Mech. Dev. 120, 561-572.

Dan-Sohkawa, M., Satoh, N., 1978. Studies on dwarf larvae developed from isolated blastomeres of the starfish, *Asterina pectinifera*. J. Embryol. Exp. Morphol. 46, 171-185.

Danilchik, M.V., Black, S.D., 1988. The first cleavage plane and the embryonic axis are determined by separate mechanisms in Xenopus laevis. I. Independence in undisturbed embryos. Dev. Biol. 128, 58-64.

Davidson, E.H., 1990. How embryos work: a comparative view of diverse modes of cell fate specification. Development 108, 365-89.

Davidson, E.H., Cameron, R.A., Ransick, A.R., 1998. Specification of cell fate in the sea urchin embryo: summary and some proposed mechanisms. Dev. Biol. 125, 3269-3290.

Davidson, E.H., Rast, J.P., Oliveri, P., Ransick, A., Calestani, C., Yuh, C.H., Minokawa, T., Amore, G., Hinman, V., Arenas-Mena, C., Otim, O., Brown, C.T., Livi, C.B., Lee, P.Y., Revilla, R., Rust, A.G., Pan, Z., Schilstra, M.J., Clarke, P.J., Arnone, M.I., Rowen, L., Cameron, R.A., McClay, D.R., Hood, L., Bolouri, H., 2002. A genomic regulatory network for development. Science 295, 1669-1678.

Driesch, H., 1892. Entwicklungsmechanische Studien III-IV. Z. Wiss. Zool. 55, 1-62.

Duboc, V., Rottinger, E., Besnardeau, L., Lepage, T., 2004. Nodal and BMP2/4 signaling organizes the oral-aboral axis of the sea urchin embryo. Dev. Cell. 6, 397-410.

Emily-Fenouil, F., Ghiglione, C., Lhomond, G., Lepage, T., Gache, C., 1998.
GSK3beta/shaggy mediates patterning along the animal-vegetal axis of the sea urchin embryo. Development 125, 2489-98.

Endo, Y., 1966. Fertilization, cleavage and early development. In Isemura, T., *et al*. (Eds.), Contemporary Biology, vol. 4, Development and Differentiation, Iwanami Shoten, Tokyo, pp. 1-61.

Erwin, D.H., 1993. The great Paleozoic crisis: life and death in the Permian. Columbia University Press, New York.

Ettensohn, C.A., Sweet, H.C., 2000. Patterning the early sea urchin embryo. Curr. Top. Dev. Biol. 50, 1-44.

Flowers, V.L., Courteau, G.R., Poustka, A.J., Weng, W., Venuti, J.M., 2004. Nodal/activin signaling establishes oral-aboral polarity in the early sea urchin embryo. Dev. Dyn. 231, 727-40.

Freeman, G., 1993. Regional specification during embryogenesis in the articulate brachiopod *Terebratalia*. Dev. Biol. 160, 196-213.

Freeman, G., Martindale, M.Q., 2002. The origin of mesoderm in phoronids. Dev. Biol. 252, 301-311.

Gerhart, J., Kirschner, M., 1997. Cells, Embryos, and Evolution: Toward a Cellular and Developmental Understanding of Phenotypic Variation and Evolutionary Adaptability. Blackwell Science, Boston.

Gross, J.M., McClay, D.R., 2001. The role of Brachyury (T) during gastrulation movements in the sea urchin Lytechinus variegatus. Dev. Biol. 239, 132-47.

Hardin, J., 1988. The role of secondary mesenchyme cells during sea urchin gastrulation studied by laser ablation. Development 103, 317-24.

Hardin, J., Coffman, J.A., Black, S.D., McClay, D.R., 1992. Commitment along the dorsoventral axis of the sea urchin embryo is altered in response to NiCl2. Development 116, 671-85.

Hardin, J., McClay, D.R., 1990. Target recognition by the archenteron during sea urchin gastrulation. Dev. Biol. 142, 86-102.

Hedgepeth, C.M., Conrad, L.J., Zhang, J., Huang, H.C., Lee, V.M., Klein, P.S., 1997. Activation of the Wnt signaling pathway: a molecular mechanism for lithium action. Dev. Biol. 185, 82-91.

Henry, J.J., Klueg, K.M., Raff, R.A., 1992. Evolutionary dissociation between cleavage, cell lineage and embryonic axes in sea urchin embryos. Development 114, 931-938.

Henry, J.J., Raff, R.A., 1990. Evolutionary change in the process of dorsoventral axis determination in the direct developing sea urchin, *Heliocidaris erythrogramma*. Dev. Biol. 141, 55-69.

Henry, J.J., Wray, G.A., Raff, R.A., 1990. The dorsoventral axis is specified prior to first cleavage in the direct developing sea urchin *Heliocidaris erythrogramma*. Development 110, 875-884.

Henry, J.Q., Tagawa, K., Martindale, M.Q., 2001. Deuterostome evolution: early development in the enteropneust hemichordate, *Ptychodera flava*. Evol. Dev. 3, 375-390.

Hinman, V.F., Davidson, E.H., 2003a. Expression of a gene encoding a Gata

transcription factor during embryogenesis of the starfish *Asterina miniata*. Gene

Expr. Patterns 3, 419-422.

Hinman, V.F., Davidson, E.H., 2003b. Expression of AmKrox, a starfish ortholog of a

sea urchin transcription factor essential for endomesodermal specification. Gene

Expr. Patterns 3, 423-426.

Hinman, V.F., Nguyen, A.T., Cameron, R.A., Davidson, E.H., 2003a. Developmental

gene regulatory network architecture across 500 million years of echinoderm

evolution. Proc Natl Acad Sci U S A 100, 13356-13361.

Hinman, V.F., Nguyen, A.T., Davidson, E.H., 2003b. Expression and function of a

starfish Otx ortholog, AmOtx: a conserved role for Otx proteins in endoderm

development that predates divergence of the eleutherozoa. Mech. Dev. 120, 1165-

1176.

Hodor, P.G., Ettensohn, C.A., 1998. The dynamics and regulation of mesenchymal cell

fusion in the sea urchin embryo. Dev. Biol. 199, 111-124.

Hörstadius, S., 1935. Über die Determination im Verlaufe der Eiachse beir Seeigeln.

Pubbl. Staz. Zool. Napoli 14, 251-479.

Hörstadius, S., 1973. Experimental Embryology of Echinoderms, Clarendon Press,

Oxford.

Hörstadius, S., Wolsky, A., 1936. Studien uber die determinationder bilateral-symmetrie

des jugen Seeigel Kimes. Wilhelm Roux's Arch. Dev. Biol. 135, 69-113.

Huang, L., Li, X., El-Hodiri, H.M., Dayal, S., Wikramanayake, A.H., Klein, W.H., 2000. Involvement of Tcf/Lef in establishing cell types along the animal-vegetal axis of sea urchins. Dev. Genes. Evol. 210, 73-81.

Hyman, L.H., 1955. The Invertebrates: Echinodermata (Vol. IV), McGraw-Hill, New York.

Imai, K., Takada, N., Satoh, N., Satou, Y., (beta)-catenin mediates the specification of endoderm cells in ascidian embryos. Development 127, 3009-20.

Kenny, A.P., Kozlowski, D., Oleksyn, D.W., Angerer, L.M., Angerer, R.C., 1999. SpSoxB1, a maternally encoded transcription factor asymmetrically distributed among early sea urchin blastomeres. Development. 126, 5473-83.

Kenny, A.P., Oleksyn, D.W., Newman, L.A., Angerer, R.C., Angerer, L.M., 2003. Tight regulation of SpSoxB factors is required for patterning and morphogenesis in sea urchin embryos. Dev. Biol. 261, 412-25.

Kiehart, D.P., 1982. Microinjection of echinoderm eggs: apparatus and procedures. Methods Cell. Biol. 25 Pt B, 13-31.

Klein, P.S., Melton, D.A., 1996. A molecular mechanism for the effect of lithium on development. Proc. Natl. Acad. Sci. USA. 93, 8455-9.

Kominami, T., 1983. Establishment of embryonic axes in larvae of the starfish, *Asterina pectinifera*. J. Embryol. Exp. Morphol. 75, 87-100.

Kominami, T., 1984. Allocation of mesendodermal cells during early embryogenesis in the starfish, *Asterina pectinifera*. J. Embryol. Exp. Morphol. 84, 177-190.

Kühn, A. 1971. Lectures on Developmental Physiology, Second Edition. Springer-
Verlag, New York, pp.166-182.

Li, X., Wikramanayake, A.H., Klein, W.H., Requirement of SpOtx in cell fate decisions
in the sea urchin embryo and possible role as a mediator of beta-catenin signaling.
Dev. Biol. 212, 425-39.

Littlewood, D.T.J., Smith, A.B., Clough, K.A., Emson, R.H., 1997. The interrelationships
of the echinoderm classes: morphological and molecular evidence. Biol. J. Linn.
Soc. 61, 409-438.

Logan, C.Y., McClay, D.R., 1997. The allocation of early blastomeres to the ectoderm
and endoderm is variable in the sea urchin embryo. Development 124, 2213-2223.

Logan, C.Y., Miller, J.R., Ferkowicz, M.J., McClay, D.R., 1999. Nuclear beta-catenin is
required to specify vegetal cell fates in the sea urchin embryo. Development 126,
345-57.

Maruyama, Y.K., Shinoda, M., 1990. Archenteron-forming capacity in the blastomeres
isolated from the eight-cell stage embryos of the starfish, *Asterina pectinifera*.
Dev. Grow. Diff. 32, 73-84.

McGadey, J., 1970. A tetrazolium method for non-specific alkaline phosphatase.
Histochemie. 23, 180-184.

Melton, D.A., 1991. Pattern formation during animal development. Science 252, 234-41.

Miller, J.R., McClay, D.R., 1997. Changes in the pattern of adherens junction-associated
beta-catenin accompany morphogenesis in the sea urchin embryo. Dev. Biol. 192,
310-22.

Miller, J.R., Moon, R.T., 1996. Signal transduction through beta-catenin and
specification of cell fate during embryogenesis. Genes. Dev. 10, 2527-39.

Miyawaki, K., Yamamoto, M., Saito, K., Saito, S., Kobayashi, N., Matsuda, S., 2003.
Nuclear localization of beta-catenin in vegetal pole cells during early
embryogenesis of the starfish *Asterina pectinifera*. Dev. Growth Differ. 45, 121-
128.

Morgan, T.H., Spooner, G.B., 1909. The polarity of the centrifuged egg. Arch. Entmech.
Org. 28, 104-117.

Morris, V.B., 1995. Apluteal development of the sea urchin *Holopneustes purpurescens*
Agassiz (Echinodermata: Echinoidea: Euechinoidea). Zool. J. Linn. Soc. 114,
349-364.

Nocente-McGrath, C., McIsaac, R., Ernst, S.G., 1991. Altered cell fate in LiCl-treated
sea urchin embryos. Dev. Biol. 147, 445-50.

Okazaki, K., 1975. Spicule formation by isolated micromeres of the sea urchin embryo.
Amer. Zool. 15, 567-581.

Olsen, H., 1942. The development of the brittle star *Ophiopholis aculeata* (O Fr. Muller),
with a short report of the outer hyalin layer. Bergens Mus. Arb. (Naturvit. Rekke)
6, 1-107.

Pease, D.C., 1939. An analysis of the factors of bilateral determination in centrifuged
echinoderm embryos. J. Exp. Zool. 80, 225-247.

Raff, R.A., 1996. The shape of life: genes, development and the evolution of animal
form. University of Chicago Press, Chicago.

Raff, R.A., 1999. Cell lineages in larval development and the evolution of echinoderms. In: Wake, M.H., Hall, B.K. (Eds.), The Origin and Evolution of Larval Froms, Academic Press, San Diego, pp. 255-273.

Range, R.C., Venuti, J.M., McClay, D.R., 2005. LvGroucho and nuclear beta-catenin functionally compete for Tcf binding to influence activation of the endomesoderm gene regulatory network in the sea urchin embryo. Dev. Biol. 279, 252-67.

Ransick, A., Davidson, E.H., 1993. A complete second gut induced by transplanted micromeres in the sea urchin embryo. Science 259, 1134-1138.

Ransick, A., Davidson, E.H., 1995. Micromeres are required for normal vegetal plate specification in sea urchin embryos. Development 121, 3215-22.

Rocheleau, C.E., Downs, W.D., Lin, R., Wittmann, C., Bei, Y., Cha, Y.H., Ali, M., Priess, J.R., Mello, C.C., 1997. Wnt signaling and an APC-related gene specify endoderm in early C. elegans embryos. Cell 90, 707-16.

Scouras, A., Beckenbach, K., Arndt, A., Smith, M.J., 2004. Complete mitochondrial genome DNA sequence for two ophiuroids and a holothuroid: the utility of protein gene sequence and gene maps in the analyses of deep deuterostome phylogeny. Mol. Phylogenet. Evol. 31, 50-65.

Scouras, A., Smith, M.J., 2001. A novel mitochondrial gene order in the crinoid echinoderm *Florometra serratissima*. Mol. Biol. Evol. 18, 61-73.

Sherwood, D.R., McClay, D.R., 1997. Identification and localization of a sea urchin Notch homologue: insights into vegetal plate regionalization and Notch receptor regulation. Development 124, 3363-3374.

Sherwood, D.R., McClay, D.R., 1999. LvNotch signaling mediates secondary mesenchyme specification in the sea urchin embryo. Development 126, 1703-1713.

Sherwood, D.R., McClay, D.R., 2001. LvNotch signaling plays a dual role in regulating the position of the ectoderm-endoderm boundary in the sea urchin embryo. Development 128, 2221-2232.

Shirai, H., Kanatani, H. 1980. Effect of local application of 1-methyladenine on the site of polar body formation in starfish oocyte. Develop. , Growth and Differ. 22, 555-560.

Smith, A.B., 1988. Fossil evidence for the relationships of extant echinoderm classes and their time of divergence. In: Paul, C.R.C., Smith, A.B. (Eds.), Echinoderm Phylogeny and Echinoderm Evolutionary Biology, Oxford Scientific Publications, Oxford, pp. 85-97.

Smith, A.B., 1997. Echinoderm phylogeny: how congruent are morphological and molecular estimates? In: Waters, J., Maples, C. (Eds.), Geobiology of Echinoderms, Paleontological Society Special Publication 3, pp. 337-354.

Smith, M.J., Arndt, A., Gorski, S., Fajber, E., 1993. The phylogeny of echinoderm classes based on mitochondrial gene arrangements. J. Mol. Evol. 36, 545-54.

Stambolic, V., Ruel, L., Woodgett, J.R., 1996. Lithium inhibits glycogen synthase kinase-3 activity and mimics wingless signalling in intact cells. Curr. Biol. 6, 1664-8.

Sumrall, C.D., Sprinkle, J., 1998. Phylogenetic analysis of living Echinodermata based on primitive fossil taxa. In: Mooi, R., Telford, M. (Eds.), Echinoderms: San Francisco, Balkema, Rotterdam, pp. 81-87.

Sweet, H.C., Gehring, M., Ettensohn, C.A., 2002. LvDelta is a mesoderm-inducing signal in the sea urchin embryo and can endow blastomeres with organizer-like properties. Development 129, 1945-1955.

Sweet, H.C., Hodor, P.G., Ettensohn, C.A., 1999. The role of micromere signaling in Notch activation and mesoderm specification during sea urchin embryogenesis. Development 126, 5255-5265.

Thorpe, C.J., Schlesinger, A., Carter, J.C., Bowerman, B., 1997. Wnt signaling polarizes an early C. elegans blastomere to distinguish endoderm from mesoderm. Cell 90, 695-705.

Vonica, A., Weng, W., Gumbiner, B.M., Venuti, J.M., 2000. TCF is the nuclear effector of the beta-catenin signal that patterns the sea urchin animal-vegetal axis. Dev. Biol. 217, 230-43.

Weitzel, H.E., Illies, M.R., Byrum, C.A., Xu, R., Wikramanayake, A.H., Ettensohn, C.A., 2004. Differential stability of beta-catenin along the animal-vegetal axis of the sea urchin embryo mediated by dishevelled. Development 131, 2947-56.

Whittaker, J.R., Meedel, T.H., 1989. Two histospecific enzyme expressions in the same cleavage-arrested one-celled ascidian embryos. J. Exp. Zool. 250, 168-175.

Wikramanayake, A.H., Huang, L., Klein, W.H., 1998. beta-Catenin is essential for patterning the maternally specified animal-vegetal axis in the sea urchin embryo. Proc. Natl. Acad. Sci. USA. 95, 9343-8.

Wikramanayake, A.H., Hong, M., Lee, P.N., Pang, K., Byrum, C.A., Bince, J.M., Xu, R., Martindale, M.Q., 2003. An ancient role for nuclear beta-catenin in the evolution of axial polarity and germ layer segregation. Nature 426, 446-50.

Wikramanayake, A.H., Peterson, R., Chen, J., Huang, L., Bince, J.M., McClay, D.R., Klein, W.H., 2004. Nuclear beta-catenin-dependent Wnt8 signaling in vegetal cells of the early sea urchin embryo regulates gastrulation and differentiation of endoderm and mesodermal cell lineages. Genesis 39, 194-205.

Winchell, C.J., Sullivan, J., Cameron, C.B., Swalla, B.J., Mallatt, J., 2002. Evaluating hypotheses of deuterostome phylogeny and chordate evolution with new LSU and SSU ribosomal DNA data. Mol. Biol. Evol. 19, 762-76.

Wolpert, L., Gustafson, T., 1961. Studies on the cellular basis of morphogenesis of the sea urchin embryo. Development of the skeletal pattern. Exp. Cell Res. 25, 311-25.

Wray, G.A., Raff, R.A., 1989. Evolutionary modification of cell lineage in the direct-developing sea urchin *Heliocidaris erythrogramma*. Dev. Biol. 132, 458-470.

Wray, G.A., Raff, R.A., 1990. Novel origins of lineage founder cells in the direct-developing sea urchin *Heliocidaris erythrogramma*. Dev. Biol. 141, 41-54.

Zito, F., Tesoro, V., McClay, D.R., Nakano, E., Matranga, V., 1998. Ectoderm cell--

    ECM interaction is essential for sea urchin embryo skeletogenesis. Dev. Biol.

    196, 184-92.

Vita

Alexander Edward Primus was born in Oklahoma City, Oklahoma on June 21, 1976, the son of Jannine Gauthier Primus and John Edward Primus. After graduating from Edina High School in Edina, Minnesota in 1994, he entered the University of Colorado at Boulder where he stayed until the spring of 1997. Alex completed his undergraduate studies in biology at Carleton College in Northfield, Minnesota in 1999. Alex then moved to Seattle, Washington where he worked for a year and applied to graduate schools. In the fall of 2000 he entered graduate school at the University of Texas at Austin.

Permanent address: 6716 Arrowhead Pass, Edina, MN 55439

This dissertation was typed by the author.